SIGNIFICANCE OF QT DISPERSION AS A DIAGNOSIS TOOL FOR CARDIAC PATIENTS

A THESIS

SUBMITTED TO THE DEPARTMENT OF ELECTRICAL AND

ELECTRONICS ENGINEERING

AND THE INSTITUTE OF ENGINEERING AND SCIENCES

OF BILKENT UNIVERSITY

IN PARTIAL FULFILLMENT OF THE REQUIREMENTS

FOR THE DEGREE OF

MASTER OF SCIENCE

By

Nabil Ben Ahmed Jemel

February 2000

I certify that I have read this thesis and that in my opinion it is fully adequate, in scope and in quality, as a thesis for the degree of Master of Science.

Prof. Dr. Hayrettin Köymen(Supervisor)

I certify that I have read this thesis and that in my opinion it is fully adequate, in scope and in quality, as a thesis for the degree of Master of Science.

Prof. Dr. Yusuf Ziya İder

I certify that I have read this thesis and that in my opinion it is fully adequate, in scope and in quality, as a thesis for the degree of Master of Science.

Prof. Dr. Enis Çetin

Approved for the Institute of Engineering and Sciences:

Prof. Dr. Mehmet Baray
Director of Institute of Engineering and Sciences

ABSTRACT

SIGNIFICANCE OF QT DISPERSION AS A DIAGNOSIS TOOL FOR CARDIAC PATIENTS

Nabil Ben Ahmed Jemel
M.S. in Electrical and Electronics Engineering
Supervisor: Prof. Dr. Hayrettin Köymen
February 2000

Electrocardiogram (ECG) is the recorded electrical potentials generated by the heart during a cardiac cycle. Cardiac abnormalities cause unknown current flows leading to strange waveform morphologies in the recorded ECG. Some of these abnormalities are only visible when the heart is under stress. Exercise ECG is conducted for this reason.

Ischemia is one of the important cardiac abnormalities and is the focus of our study. It occurs when a part of the heart tissue dies or is injured. QT dispersion (QTd) is a proposed method for diagnosing Ischemia. The classical definition for QTd is the difference between the maximum and the minimum QT intervals within the 12 leads.

In this study the effect of exercise on QT dispersion (QTd) is studied and whether QTd could give significant information for diagnosing patients with ischemic heart disease is investigated. A new method for measuring QT interval

is developed and is compared with previous methods. QTd is measured on average beats calculated for 10 seconds intervals throughout the exercise ECG test and a trend curve which we call QTd, is generated. Several decision rules for the diagnosis of cardiac patients are proposed by analyzing these QTd trend curves and the accompanying heart rate curves. It is shown that despite the improvement in QT interval measurements, none of the decision rules proved to be a clinically useful discriminate of cardiac patients, with sufficient confidence.

Keywords:Exercise ECG, QT interval, QT dispersion, Ischemia.

ÖZET

EGZERSİZ TESTİ SIRASINDA ÖLÇÜLEN QT DAĞILIMININ KALP HASTALIKLARININ TEŞHİSİNDEKİ ÖNEMİ

Nabil Ben Ahmed Jemel
Elektrik ve Elektronik Mühendisliği Bölümü Yüksek Lisans
Tez Yöneticisi: Dr. Hayrettin Köymen
Şubat 2000

Elektrokardiyogram(EKG), kalp tarafından bir kalp atımı sırasında oluşturulan elektriksel potansiyallerin kaydedilmiş halidir. Kalpteki anormallikler sıradışı elektrik akımlarının akmasına neder olurlar ki, bu da kaydedilen EKG'de olağandışı morfolojiler olarak gözlenir. Bu morfolojilerin bazıları sadece kalp stres altındayken gözlenebilir. Egzersiz (Stres) EKG testi bu amaçla uygulanır.

Çalışmamıza konu olan iskemik bozukluklar en önemli kardiyolojik bozukluklardandır. Bu durum kalp dokusunun bir bölümü öldüğünde veya zarar gördüğünde ortaya çıkar. QT dağılımı (QTd) iskemik bozuklukları teşhis etmek için önerilen bir yöntemdir. QTd, en bilinen şekliyle, standart 12 EKG kanalı içinde en uzun ve en kısa QT aralıkları arasındaki fark olarak tanımlanır.

Araştırmamızda egzersiz EKG testinin QTd üzerine etkisini incelenmiş ve bundan iskemik bozuklukların teşhisinde kullanılabilecek önemli bir bilgi elde

edilip edilemediğine bakılmıştır. Bu çalışma sırasında QT aralığını ölçmek için yeni bir yöntem geliştirilmiş ve eski yöntemlerle karşılaştırılmıştır. QTd her 10 saniyede bir hesaplanan averaj EKG sinyali (bir kalp atımı) üzerinde bu yöntem kullanılarak ölçülmüştür. Bu ölçümlerden zamana bağlı bir QTd eğrisi (QTd trend) çizilmiştir. QTd ve kalp hızı eğrileri kullanılarak, iskemik bozuklukların teşhisi için değişik yöntemler önerilmiştir.

Bu çalışmamız göstermiştir ki, QT aralığı ölçümlerindeki iyileşmeye karşın önerilen yöntemlerden hiçbiriyle, QTd eğrilerinin kardiyolojik bozuklukların teşhisinde klinik değer taşıdığı gösterilememiştir.

Anahtar Kelimeler: QT aralığı, EKG, QT dağılımı, Egzersiz EKG testi, Stres EKG testi, İskemik bozukluklar

ACKNOWLEDGMENTS

I would like to express my deep gratitude to Dr. Hayrettin Köymen for his supervision, guidance, suggestions and encouragement through the development of this thesis.

I would like to thank Dr. Enis Çetin and Dr. Yusuf Ziya İder for reading and commenting on the thesis.

I am intended to Fikret Küçükdeveci and Mustafa Solmaz from TEPA Ltd co. for their assistance in data acquisition. I would like to express my appreciation to Burak Acar, Lutfu Ozcakir and to all my friends inside and outside the department for their continuous support through the development of this thesis.

Finally, I would like to thank my family, especially my parents and my uncle, for their continuous support along my studies.

Contents

List of Figures

List of Tables

To my Family ...

Chapter 1

INTRODUCTION

The electrical structure of the heart can be divided into three major components: Pacemaker cells, specialized conduction tissue and working muscle of the artria and ventricals.

A cardiac cycle starts normally in the pacemaker cells, which are located in the SA node. These cells are self-excitatory and thus provide a regular succession of action potentials. These action potentials stimulate the cells in the left and right artria and result in a wave of cellular depolarization, which cause the artria to contract and fill the ventricles with blood. When this excitation reaches the AV node a specialized conduction tissue transmits the excitation to the ventricles. This specialized tissue is characterized by its low conductivity; this results in a delay between ventricular and arterial excitation.

In the ventricular regions the HIS-Purkinje tissue transmits the action potential to different parts of the left and right ventricles then the action potential is further transmitted throughout the ventricle muscle on a cell to cell basis leading to the ventricular contraction.

The cardiac electrical activity can be observed in the electrocardiogram

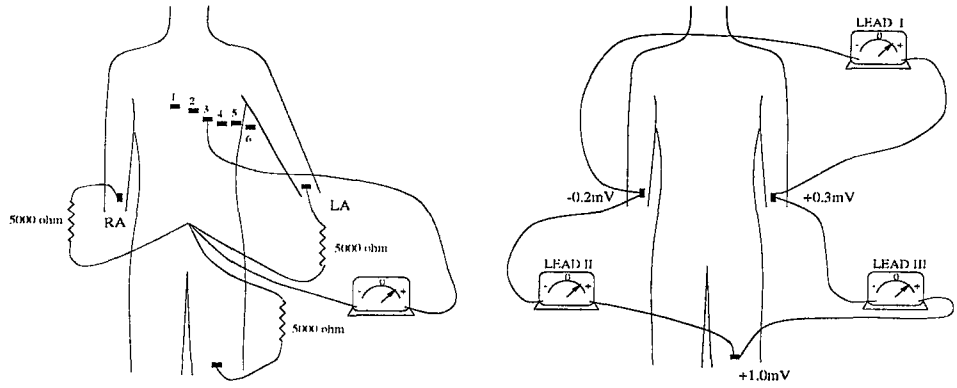

Figure 1.1: Standard leads used in ECG recording.

(ECG). ECG is the recorded electrical potentials on the surface of the body generated by the heart during a cardiac cycle. The ECG is measured using leads connected to the body surface. The standard leads (I, II, III) were originally introduced by Einthoven [3]. These leads are connected to the extremities (wrists and ankles) (Figure 1.1).

A typical lead voltage as function of time is shown in Figure 1.2. It is com-

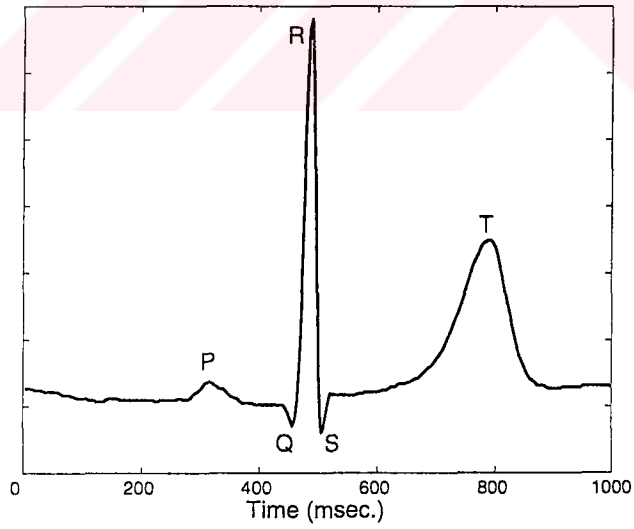

Figure 1.2: A typical heart beat.

posed of a P wave, a QRS complex and a T wave. The P wave corresponds to the activation of the artria. The repolarization of the artria is usually masked by the QRS complex, which corresponds to the depolarization of the ventricles. The repolarization of the ventricles is reflected in the T wave. The QT interval gives the total duration of the ventricular systole. It is defined as the time interval between the onset of QRS complex and the end of T wave (Figure 1.2). This interval is widely recognized as an index of ventricular repolarisation. The QT interval varies between the 12 leads (Figure 1.3). This

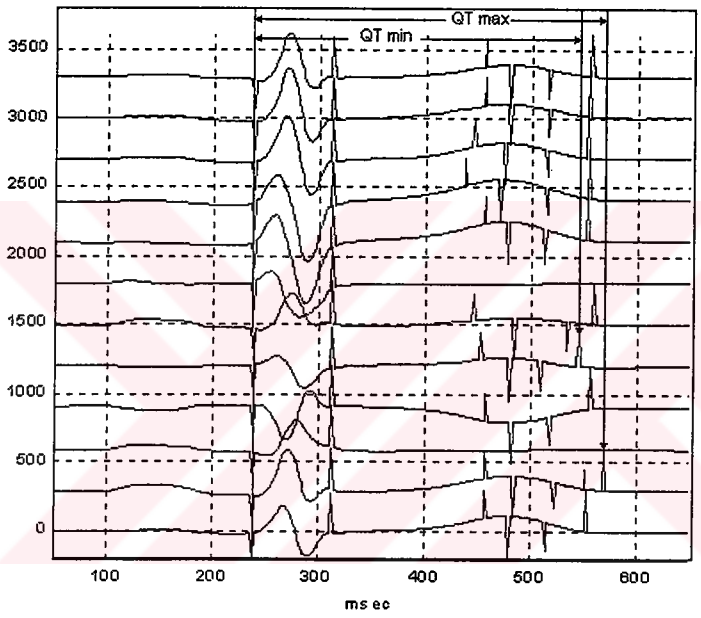

Figure 1.3: QT interval variation within the 12 leads.

inter-lead variation, known as QT dispersion (QTd) has been proposed as an index of heterogeneity of the repolarization within the ventricles of the heart. This concept (QTd) was first introduced in 1990 by Day et al. [8] for assessing patients with long QT syndrome. The definition of QT dispersion varied between different studies. The most common definition is the difference between the longest and the shortest QT interval among the 12 leads (also referred to as

12-lead range). Other studies used the standard deviation of the QT interval in 12 leads , coefficient of variation(standard deviation/mean) ,QT dispersion ratio (QT dispersion/cycle length) ,and interquartile range(difference between the upper and lower quartiles of measured QT intervals) . Table 1.1 provides a set of publications where these formulae have been used.

QT dispersion was a subject of interest by clinical cardiologists because it

Reference	Formula
Langley et al. [15]	Range, Standard deviation, Interquartile range
Higham et al. [12]	Range, Dispersion ratio
Bhullar et al. [11]	Range, Coefficient of variation
Davey et al. [13]	Range, Standard deviation, 10 lead range
Hnatkova et al. [14]	Range, Standard deviation, 10 lead range

Table 1.1: Published QT dispersion Measurement Methods

is hypothesized that QT dispersion is associated with high-risk arrhythmia, infarction, hypertrophic cardiomyopathy and other cardiac diseases. This was based on the idea that QT dispersion could reflect a regional heterogeneity of myocardial recovery. However the significance of QT dispersion as a noninvasive diagnosis tool for cardiac abnormalities is still a subject of discussion. Previous studies have shown that the measurements of QT dispersion from resting ECG were often not discriminative between patients at high and low risk of cardiac events after myocardial infarction. Stoletniy et al. [4] proposed that exercise-induced QTd may be useful in distinguishing patients with coronary artery disease from those with angiographically normal coronary arteries. QT_c is derived in order to reduce the effect of heart rate increase and compare the measurements, which have been done at different heart rates. The frequently used formulas for QT_c are Bazett's formula (1.1) and Framingham

Heart Study QT interval correction formula(1.2).

$$QT_c = QT + \frac{QT}{\sqrt{RR_{int}}} \tag{1.1}$$

$$QT_c = QT + 0.154(1 - RR_{int}) \tag{1.2}$$

Stoletniy et al. have demonstrated that patients with significant coronary artery disease had a significant increase in QT_c dispersion compared with patients who had normal exercise test results and low probability of coronary artery disease. However, in their study they assessed only QT_c without the original QT dispersion.

Gang Yi et al. [5] studied the effect of exercise on QT interval duration and dispersion in patients with sudden cardiac death after myocardial infarction. In their study 26 postinfarction patients were studied, 13 of whom suffered from sudden cardiac death and 13 of them remained event-free. Further 13 patients with chest pain, normal coronary arteriograms and negative exercise test results were studied as controls. QT intervals for this study were measured manually from rest, the end of peak exercise and 3 minutes after exercise. The QT intervals were measured in three consecutive QRS complexes in each lead when ever possible, and the average value was used. Gang Yi et al. found that exercise induced a prolongation of QT_c interval in patients at high risk of sudden cardiac death [5]. They explained this by the fact that ventricular repolarization fails to adapt normally to increasing heart rate in sudden death patients. However they failed to prove the hypothesis that exercise-induced ischemia may increase the QT dispersion.

Ozcakir et al. [7] studied the effect of exercise on QT dispersion. They have reported that QT dispersion increased in patients with ischemic heart disease. These patients were verified by coronary angiography (invasive diagnostic tool

for ischemic heart disease), however the number of patients with ischemic heart disease was not enough for statistical verification.

The T wave offset is the most important and the most problematic measurement for QT dispersion analysis. Tend was detected manually by cardiologists by the use of magnifiers, rulers calipers or digitizing tablets. The T-end is detected manually by fitting a line to the falling edge of the T wave. The intersection of this line with the isolectric line is defined as the T-end (Figure 1.4). In addition to its being labor intensive the T-end of T wave is often

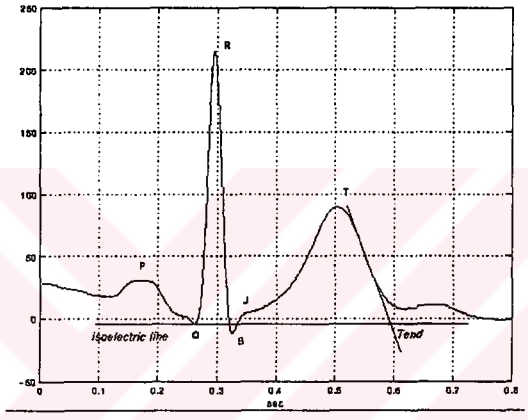

Figure 1.4: Manual T-end detection

difficult to determine manually due to the effect of noise on the falling edge of the Twave. Inter-operator differences between 10 and 28 ms have been reported [6]. All these make it necessary to develop a reliable automatic QT measurement technique not only because it is labor saving but also because it will remove subjectivity from the measurement.

Several methods were proposed for automatic T-end measurement. These methods can be classified into two major types. One based on threshold and other on maximum T wave slope (Figure 1.5). In the threshold approach three algorithms have been used:

Threshold method(TH): It searches for the Tend starting from the maximum T peak. T end is detected as the point at which the T wave amplitude falls below a certain percentage $(5 - 20\%)$ of the maximum Tpeak.

Derivative threshold method(DTH): The derivative of the signal is calculated. The maximum of the derivative after the Tpeak is determined. The T offset is located as the point at which the derivative falls to a certain percentage $(5 - 20\%)$ of its maximum value.

T wave area method(TA): The area under the T wave is calculated. Tend is determined as the point at which the area under the T wave is a certain percentage (90%) of the total area.

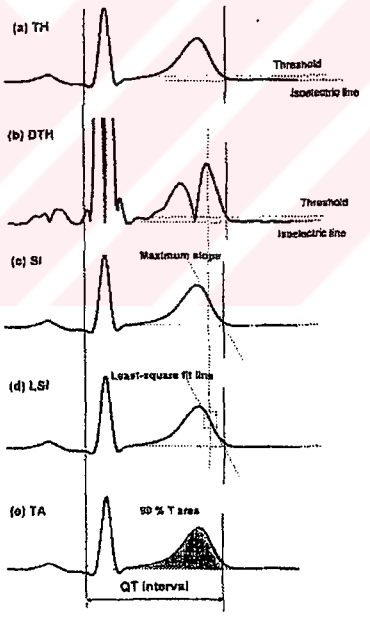

Figure 1.5: Algorithms for automatic QT interval measurement.

In the approach based on maximum slope two methods have been used:

Maximum slope method(SI): The point with maximum derivative on the falling edge of the T wave is determined. A tangential line is fitted to this point. The T offset is determined as the intersection of the maximum slope line with isoelectric line of the TP segment.

Least square fit method(LSI): A least square line is fitted around the region of the maximum slope point on the falling edge of the T wave. The intersection of this line with the isoelctric line is defined as the T-end.

Xue et al. [2] have compared these five algorithms for T offset measurements. A reproducibility test was conducted. For comparing the available algorithms test data from 23 normal subjects each of whom had five ECGs recorded was used. The repeated ECGs were obtained 30 minutes, 1 day, 1 week and one month after the first. QT dispersion was calculated for all five ECG then the median value was determined. Xue et al. defined the individual average of the four absolute differences (IDIFF) as:

$$IDIFF = \frac{1}{4}\sum_{i=1}^{4} |QTd_i - median| \tag{1.3}$$

According to this definition, a good reproducibility corresponds to a small IDIFF value. Xue et al. have reported that the least-squares fit algorithm achieved better reproducibility of QT dispersion measurements than any other method examined. It was also suggested that the least-squares fit algorithm achieved better reproducibility than the simple slope method because of more stable fitting due to more sample points.

In this study a new algorithm for automated QT measurement (LSPF) is proposed. The fiducial points detected by the algorithm were verified visually. The algorithm is then modified and improved with respect to visual detection. The performance of the algorithm is compared with previously developed algorithms (mainly with the least-squares fit algorithm)

In this study, the QT interval is measured throughout the whole exercise test. The QTd trends are then calculated using the resulting QT intervals. A new approach is presented for calculating the QTd trends. Unlike previous studies where at most three average values (rest, exercise and recovery) of QTd dispersion were calculated, in this study QTd trends are generated for the entire exercise and recovery phases. The efficiency of this new method is discussed and compared with the previously proposed methods for QTd calculation. QTd trends are generated for 24 patients, 12 of which were diagnosed cardiac using ST test. Several decision rules are proposed for classifying the different QTd trends. A sensitivity-specificity test is conducted for evaluating these decision rules and thus the performance of QTd as a diagnosis tool for cardiac patients.

Chapter 2

THE METHOD

Our algorithm can be divided into four basic blocks. A block diagram for the entire algorithm is shown on Figure 2.1. Each block is explained in detail in the following sections.

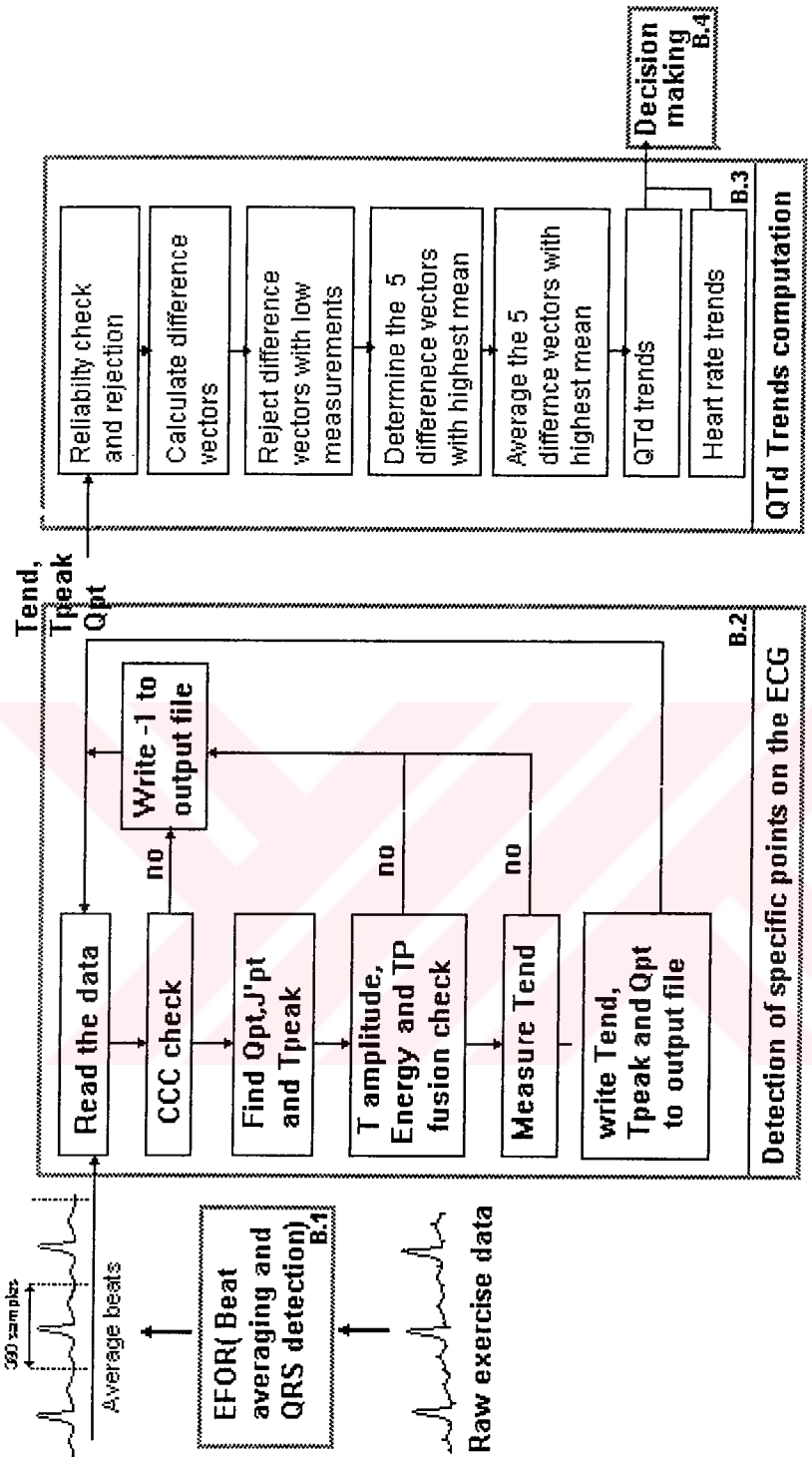

Figure 2.1: Block diagram for the algorithm.

2.1 Beat Averaging and QRS Detection

The commercially available software Efor from TEPA Ltd. is used for beat averaging and noise reduction. The Efor program provides an average beat for every 10 seconds of raw data.

It is known that the steepest change on the ECG recording occurs at R waves. For this reason a trigger point is defined as the point at which the derivative of the R wave falls to 80 % of its peak value. Using the rest data, a template, which represents a normal QRS morphology, is computed separately for each lead. Then a reference channel is determined for all the leads. The reference channel is defined as the channel that has the highest correlation with its template at rest. The calculated templates are used for QRS detection throughout the rest of the exercise data.

The exercise data is divided into 10 seconds segments. After detecting all QRS complex candidates within a segment a correlation test is made. If the correlation between a QRS complex candidate and the corresponding template is high enough the beat is qualified. The qualified beats are aligned using the ascending edge of the R wave. This results in one average beat for every 10 seconds of data. The average beats for the 12 different leads obtained are time aligned with respect to the reference channel. The length of the average beat is 380 samples. The 128th sample corresponds to its trigger point. The beats and its information are then recorded to a file.

2.2 Detection of Specific Points on the ECG

We measure the QT intervals needed for determining the QT trends on the average beats defined in the previous section. We obtain four fiducial points for each lead. They are the Q point (Qpt), J' point (Jpt'), T-peak (Tpk) and T-end (T-end) (Figure 2.2).

For determining the specific points we define different search window for each point. We define the search windows according to the characteristics of the exercise ECG. Since the trigger point which corresponds to the falling edge of the R wave is already provided (Section 2.1), it was not necessary to develop an algorithm for determining the R wave peak. In the following the trigger point is used whenever the position of the R wave is needed.

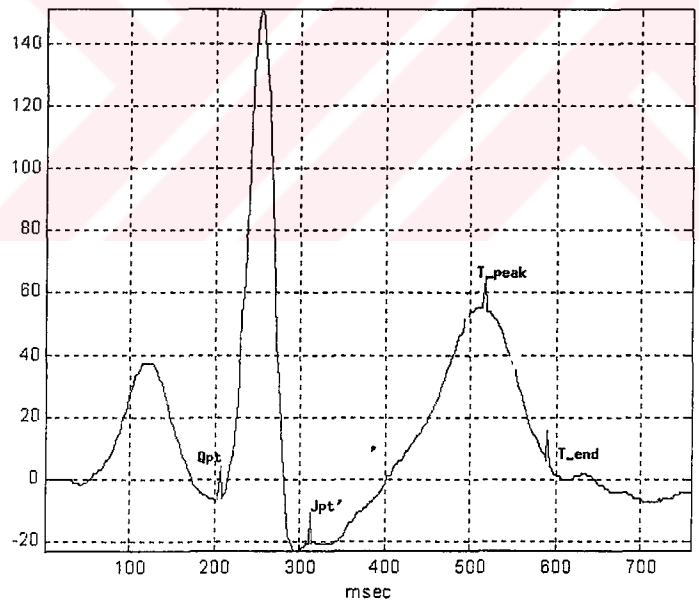

Figure 2.2: Fiducial points.

2.2.1 Q point Detection

The Q point (Qpt) is needed for the calculation of the QT intervals and the calculation of the isoelectric line (baseline1). It is known that the Q wave always proceeds the R wave. For this reason it is reasonable to start searching for the Q point before the R wave peak. In our algorithm we set the search window for the Q point to 50 ms proceeding the trigger point. It has been shown that the variance of the QRS onset across the 12 leads is very low compared to that of the T-end [2]. For this reason, knowing that all the leads are time aligned, we detect a global Q point for all 12 leads. We detect it on the reference channel as follows:

We calculate the first derivative of the average beat $d(n)$ as:

$$d(n) = \frac{|x(n) - x(n-2)|}{2} \tag{2.1}$$

We define Qpt as the first point in the search window for which $d(n) \geq 1$.

Both the search window and Qpt are shown in Figure 2.3 .

After determining the Q point we make a derivative check. Our aim from this check is to assure that the detected Q point is on the ascending edge of the R wave and not the falling edge of the P wave. Since the Q point is expected to be on the ascending edge of the R wave we expect the derivative of the five sample points after the Q point to be greater than 1. If the derivative check is negative we narrow the search window for the Q point so that to exclude the falling edge of the P wave. We then repeat the search for the Q point on the new search window.

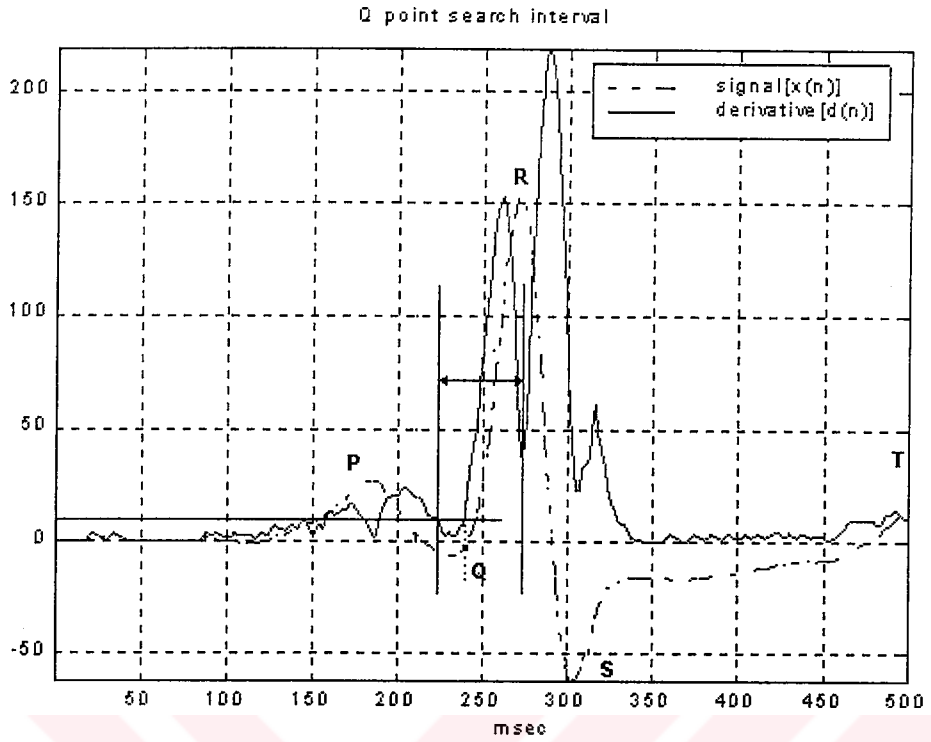

Figure 2.3: Q point detection.

2.2.2 Isolectric Line Calculation

After we determine the correct Q point, we calculate an approximation to the baseline (isoelectric line). We call it 'baseline1'. We first define a search window of length 40 milliseconds proceeding the global Q point. This window corresponds to the segment between P wave end and QRS onset. On this window we search for the 10 sample points (20 milliseconds) with the lowest standard deviation. We then calculate baseline1 as the average of these 10 sample points.

2.2.3 J point' Detection

According to [7] the QRS complex returns to its DC level 50 milliseconds after the R wave. We use this physical property of the ECG for defining J point' (Jpt'). We define a common J point' for all leads as follows:

Jpt' : $Trigger\ point\ +\ 50\ milliseconds$.

Jpt' is not the correct J point but it seemed to be reliable for marking the end of the QRS complex. We use Jpt' for calculating a second baseline, which is called *baseline2* and defined as:

$Baseline2$: $The\ average\ of\ the\ 20\ milliseconds\ following\ Jpt'$.

The relative values of baseline1 and baseline2 can be used to determine whether there is any depression or elevation in the ST segment. Such cases are typical in exercise ECG and complicate the T wave detection considerably.

2.2.4 T-peak Detection

In our study we use a threshold based detection algorithm for determining the T-peak. The advantage of using this algorithm is that it has less computation time and it is able to deal with several complications of exercise ECG such as ST depression ST elevation and TP fusion. TP fusion occurs when the heart rate increases and the RR interval between two consecutive heartbeats shortens. This leads to a fusion between the T wave and the P wave of the next beat(Figure 2.4). The degree of TP fusion depends on the heart rate and the amplitudes of the T and P waves.

We define the search window for the T-peak as:

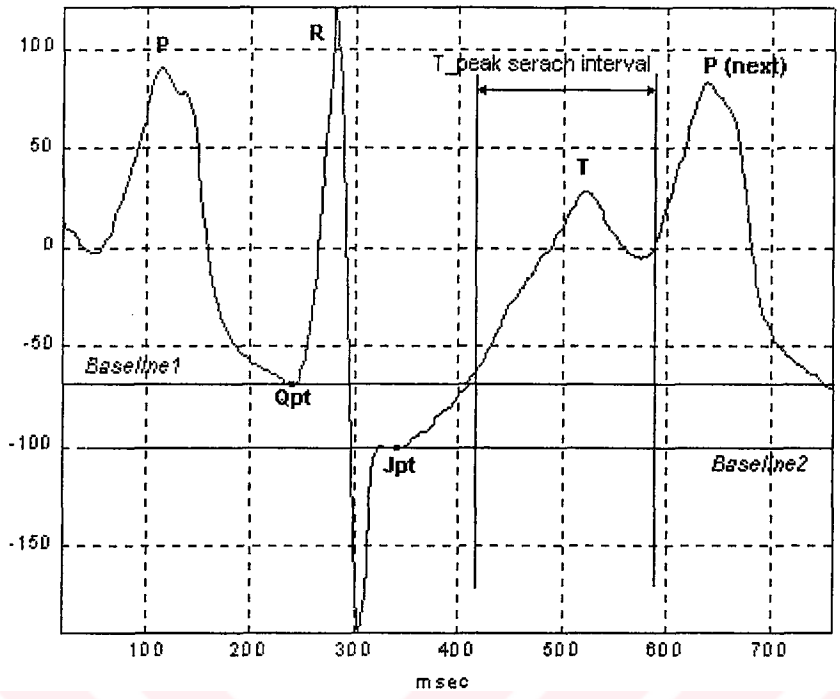

Figure 2.4: T-peak searach interval.

$$Jpt' + 80ms < t < Qpt + RRint * (2/3) + 20ms \tag{2.2}$$

It was shown in a previous study [7] that this interval excludes the P-peak of the next QRS complex. Since this interval is a function of heart beat the search range for the T-peak decreases as heart rate increases and this avoids detecting the peak of the P wave instead of that of the T wave. A TP fused beat and the corresponding search interval for the T-peak are shown on Figure 2.4 . It is clear how the search interval discards the peak of the P wave.

Once the search window for the T-peak is determined our algorithm searches for two maximums in the previously defined window . It calculates the maximums with respect to the two previously defined baselines (baseline1 and Baseline2) as follows.

*Tpeak*1 *absolute maxima with respect to baseline*1 *in the interval* (2.2.4).

*Tpeak*2 *absolute maxima with respect to baseline*2 *in the interval* (2.2.4).
In the absence of ST depression or elevation *Tpeak*1 and *Tpeak*2 are the same. If the two peaks found are different it is more likely that there is an ST depression or an ST elevation. This is checked by comparing the levels of *baseline*1 and *baseline*2

We report an ST elevation if $baseline2 > baseline1 + tol$ on the other case, if $baseline2 + tol < baseline1$, we report an ST depression. *tol* is a tolerance value which can be changed according to signal level.

For determining the correct T-peak we perform a curvature test on the detected peaks. We define an index of curvature (Cv) as follows:

$$Cv = \frac{\sum_{n=Tpk-4}^{Tpk+5} d(n)}{10} \tag{2.3}$$

Cv is the absolute average of the derivative on a 20-millisecond window around the detected T-peak. The value of Cv reflects the behavior of the signal derivative around the T-peak. We select the T-peak with highest Cv value.

2.2.5 Reliability Checks

We make several checks throughout the measurement of the QTd trend. The purpose from these checks is to determine whether the quality of the recording is good enough for QT analysis. We reject all beats that fail these checks.

Cross Correlation Coefficient Check We perform the first check on the QRS complex. We obtain 12 templates from rest ECG. These templates are simply the QRS complexes for rest ECG. We set the size of the templates to 120 milliseconds centered at the trigger point. We calculate the

cross correlation of every average beat with the corresponding template as follows.

$$CCC(n) = \frac{\sum_{i=1}^{60} x(n+i)T(i)}{\sqrt{\sum_{i=1}^{60} x^2(n+i).\sum_{i=1}^{60} T^2(i)}} \tag{2.4}$$

Where $T(i)$ is the template and $x(i)$ the input signal. The cross correlation value reflects the quality of the signal. A low SNR signal gives a low correlation between the QRS complex and the corresponding template. We accept a beat only if it has a correlation coefficient bigger than 0.7. If we accept a beat we update the corresponding template by including a fraction of the accepted beat. We perform this update as follows:

$$New\_Temp = 0.7 * old\_Temp + 0.3 * new\_QRS \tag{2.5}$$

Amplitude Checks After we determine the T-peak we perform on it an amplitude check. We set the threshold for T-peak amplitude to 0.1289 mv. We have determined this value empirically. We have tried to further decrease the value of this threshold for patients with low T wave amplitudes but this lead to a decrease in the measure accuracy. In a study on the influence of T wave amplitude on T-end measurement [10] It was reported that measurement from T waves with amplitude less than 0.25 $mvolts$ are less reliable.

Energy Check We perform an energy check to make sure that what we have detected is the peak of the T wave and not a noise spike. This check consists of measuring the energy in a window around the T-peak. The idea is that the energy in a window around a noise spike is much lower than that around the T-peak. We determine the size of the window empirically and we set to 120 $msec$. We set the threshold for passing the

energy test to 4.684 mv^2. If the measured energy under the window is less than this threshold value we reject the detected T-peak.

TP Fusion Check We check the behavior of the T wave around the T-peak in order to determine whether we have TP fusion or not. If the second half of the T wave doesn't fall to 80% of the T-peak maximum amplitude we conclude that there is a TP fusion and the beat is rejected. If the RR interval keeps decreasing (i.e. heart rate is increasing) the T-end is masked by the P wave and it will not be possible to detect it till the heart rate starts to decrease (recovery phase). It is important here to note that TP fusion is critical only for the leads where we have a small T wave compared to the P wave. The reason is that a small amplitude T wave is masked easily by the P wave leading to TP fusion rejection starting from early stages of exercise.

Whenever a beat fails in any of the above checks, we reject the beat. Otherwise, we assume that it is good enough for T-end detection.

2.2.6 T-end Detection

The T-end detection algorithm, which we use in this study, is based on a similar idea to the one used by cardiologists. The idea of this algorithm was first introduced by L.Ozcakir [7]

We model the T wave by a second-degree parabola:

$$y(t) = a * t^2 + b * t + c \tag{2.6}$$

The window to which we fit the parabola is defined as the points at which the T wave amplitude is above the 80% of its maximum around T-peak. In Figure 2.5 the T-end and the fitted parabola are shown.

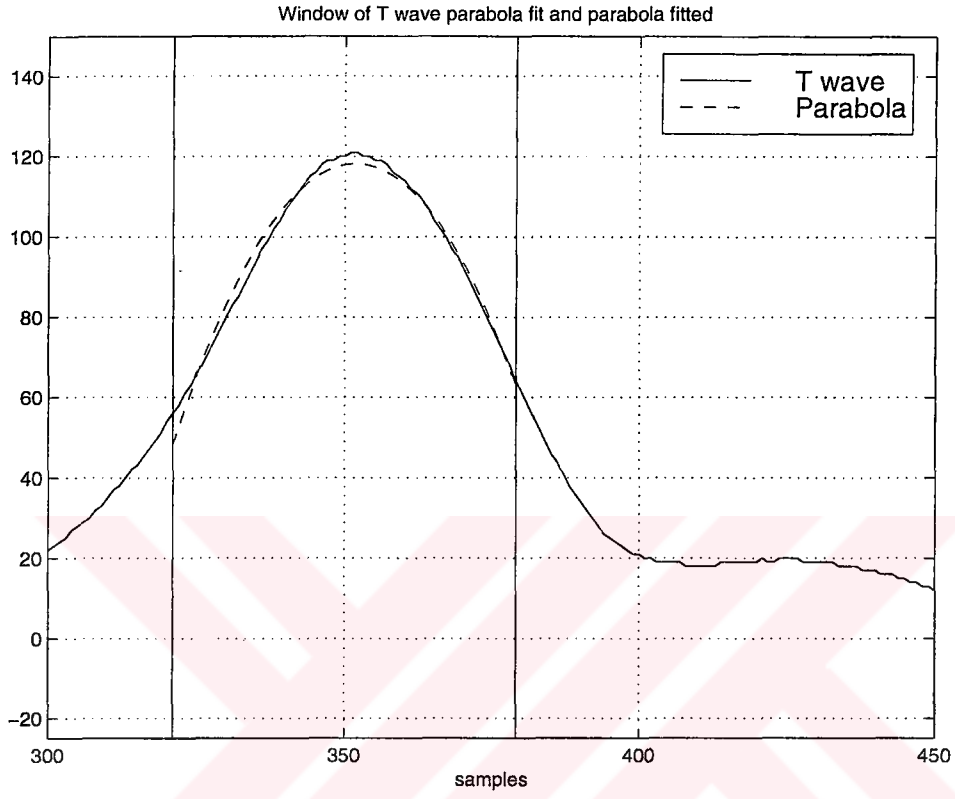

Figure 2.5: Parabola fitting to the T wave

We use the least square approximation technique for fitting the second-degree parabola. This technique minimizes the error between the signal and the fitted parabola as:

$$\min_{a,b,c} \sum_{i=1}^{l} (y_i - (a * x_i^2 + b * x_i + c))^2 \tag{2.7}$$

Where l is the length of the interval to which we fit the parabola and x_i all sample indexes within this interval. After minimizing the above equation we

obtain the following system of equations:

$$\begin{pmatrix} n & \sum x_i & \sum x_i^2 \\ \sum x_i & \sum x_i^2 & \sum x_i^3 \\ \sum x_i^2 & \sum x_i^3 & \sum x_i^4 \end{pmatrix} \begin{pmatrix} c \\ b \\ a \end{pmatrix} = \begin{pmatrix} \sum y_i \\ \sum y_i x_i \\ \sum y_i x_i^2 \end{pmatrix} \tag{2.8}$$

We use the conjugate gradient algorithm for solving this system of equations.

Once we obtain the parameters of the parabola, we determine V_{80} as the point where the fitted parabola falls to 80 % of its absolute maximum on its falling edge. We then draw the tangential line (T_{80}) through (V_{80}). Unlike the signal itself the fitted parabola is mathematically well defined and so is the tangential line. Thus the errors due to tangent line fitting to the T wave [1] are avoided. We then determine the T-end as the intersection of T_{80} with the baseline voltage level $baseline1$.

2.3 QTd Trends Computation

After determining the fiducial points the next step in our algorithm is to calculate the QT dispersion trends. The first step in this calculation is the elimination of suspicious measurements. This elimination is based on the continuity assumption: we assume that in a short interval there can be no abrupt change in the ECG features. In case any occur, we report it as an erroneous measure. Once we eliminate all suspicious measurements we calculate the QTd on the reliable leads and finally we obtain a single QTd trend.

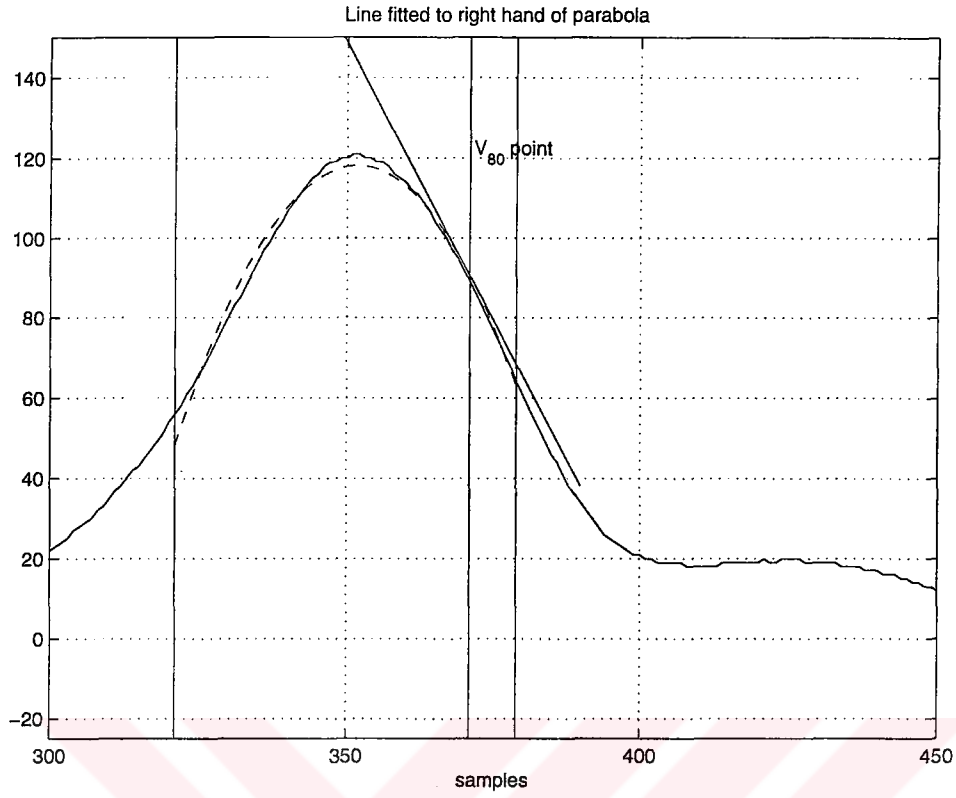

Figure 2.6: T-end detection.

2.3.1 Check for the Reliability of the Detected Points

Q point Verification In this part we check for points where we have erroneous detection of Qpt. A derivative check test is made according to the principle of continuity. We assume that the Q-point can not change by more than 10 milliseconds between two successive average beats. Assume $Qpt(n)$ is the position of Qpt in the n^{th} average beat, measured with respect to the trigger point, then $Qpt(n)' = [Qpt(n) - Qpt(n-1)]/2$ is the first order difference of this discrete signal. We eliminate the average beats that correspond to $Qpt(n)' > 5$.

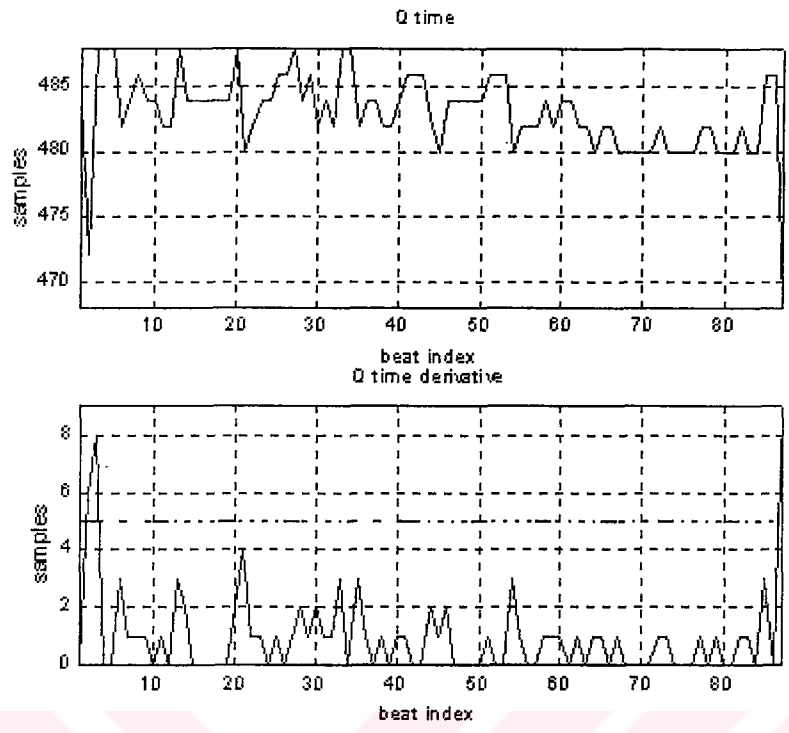

Figure 2.7: Q point elimination.

Tpeak Verification Similarly we perform a T-peak test for each lead. Unlike the $Qpt(n)$ $Tpeak_i(n)$ may show some discontinuity. These are due to the beats where measurements were not possible either due to very low amplitude T wave, or TP fusion.

Figure 2.8 shows a continuous and discontinuous $Tpeak_i$. The discontinuity in the second 2^{nd} graph is due to biphasic T waves in this example.

When a biphasic T wave exists, the T-peak detection algorithm keeps alternating between the two peaks since both peaks can qualify the derivative check (Cv) (Figure 2.8). Although the second peak of the T wave can be detected at the earlier phases of the exercise test, it is masked in later phases due to TP fusion. At this step our algorithm will start measuring the first peak. So we decided to stick to the first peak throughout

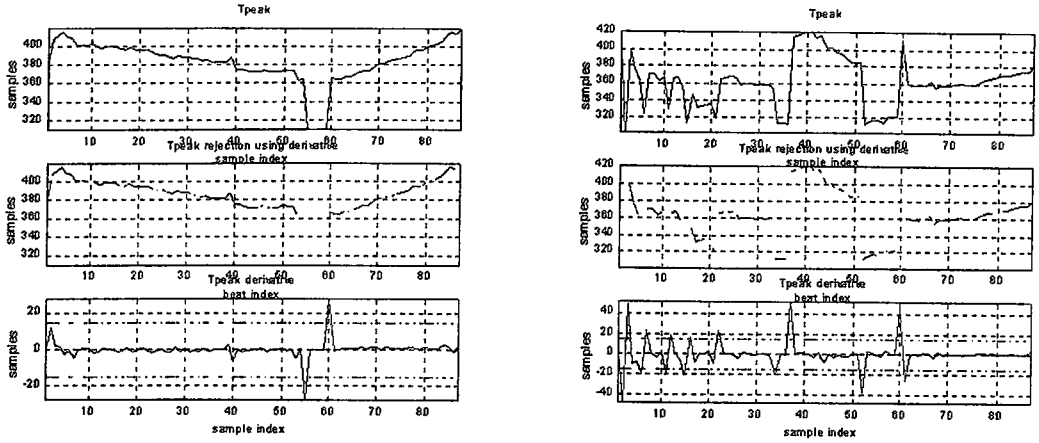

Figure 2.8: T-peak elimination.

the exercise.

We calculate the first order difference $Tpeak_i(n)' = [Tpeak_i(n) - Tpeak_i(n-1)]/2$. When $Tpeak_i(n)'$ exceeds a certain threshold (set to 15 milliseconds in our case) the measurement is eliminated. After verifying and eliminating all wrong T-peak measures we end up with 12 QTpk interval vectors one vector for each lead. A lead vector $Tpk_i(n)$ contains the valid T-peak measurements and -1s which correspond to unavailable measurements. These lead vectors are used later for calculating QTpk dispersion trends.

T-end Verification Since there is relatively a low number of measurements for the T-end compared to that of the Q point and T-peak we use a different process for eliminating the erroneous T-end measurements.

Our algorithm models the variation of the T-end in the exercise and the recovery phases of each lead by using two different second-degree parabolas. If there are more then 8 accepted T-end measurements in each phase, we fit a parabola to $Tend_i(n)$. Otherwise we reject all the

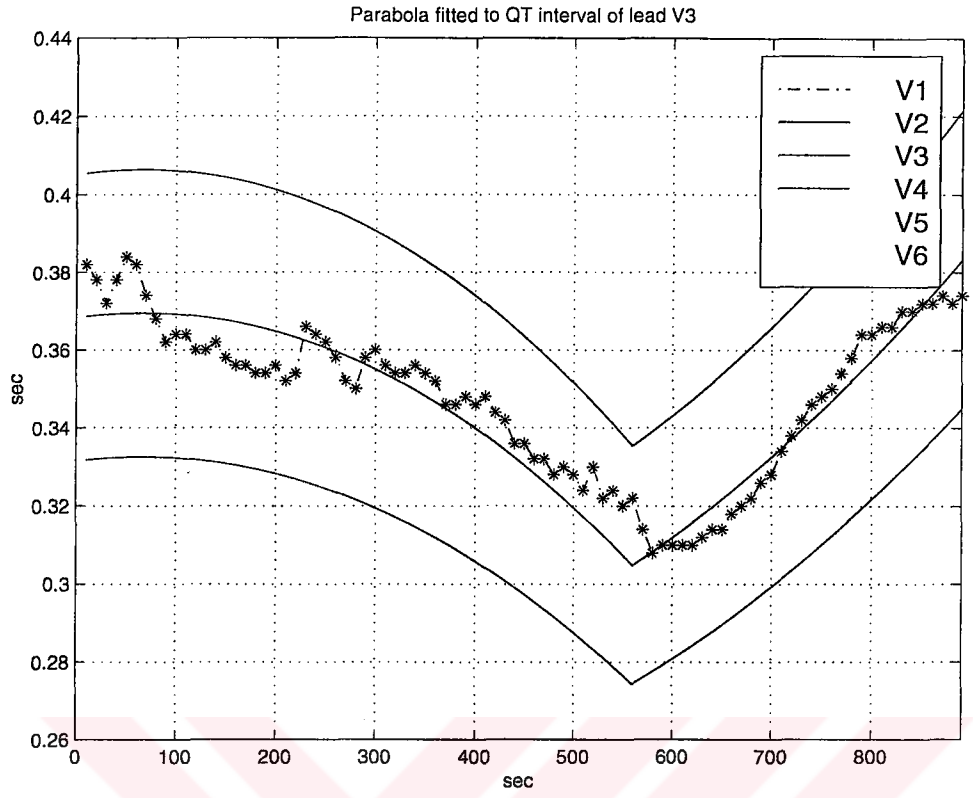

Figure 2.9: T-end elimination.

measurements within that phase. Once we fit a parabola, we reject the T-end measurements which fall out of the $\pm 8\%$ amplitude range (empirically determined) of the parabola. Thus we exclude the outliers. This rejection is also based on the continuity assumption. Figure 2.9 shows a sample $Tend_i(n)$ with the fitted parabolas in exercise and recovery phases. The $\pm 8\%$ amplitude ranges are also shown.

2.3.2 QTd Computation

After verifying and eliminating all wrong measures we end up with 12 QT interval vectors one vector for each lead. A lead vector $Tend_i(n)$ contains the valid T-end measurements and -1s which correspond to unavailable measurements. We also obtain a different set of lead vectors Tpk_i containing the valid T-peak measurements and -1s for unavailable measurements. We use this second set of calculating Q-Tpeak dispersion trends.

We define QTd vectors as:

$$QTd_{ij}(n) = \begin{cases} QT_i(n) - QT_j(n) & \text{if } QT_i(n) \neq \text{-1 and } QT_j(n) \neq \text{-1} \\ -1 & \text{o.w} \end{cases}$$

$QTd_{ij}(n)$ presents the QT interval difference between lead i and lead j for all available samples. We calculate QTd_{ij}'s for all possible pairs of leads. This results in 64 different QT different QTd_{ij}'s .

Then we divide the exercise phase into five equal segments. The fifth slice corresponds to the highest stage of exercise. The heart rate is very high at this stage and we expect a high amount of dispersion. However due to the increase in the heart rate, TP fusion at this stage is very high. As a result of this, T-end detection is difficult and not reliable. The first slice corresponds to early stages of exercise and we do not expect to observe effects of ischemia in this part. For this reason we do only consider the second, third and fourth segments of the exercise phase. Let I_s be the interval corresponding to these segments.

Despite the fact that TP fusion is low on I_s it is still possible that T-end measurements are not available due to noise or low T wave magnitude. For more reliable analyzes we decided to reject QTd_{ij}'s with less than 70% of maximum

number of possible measurements in I_s . We set our 70% threshold for lead rejection after analyzing the effect of different thresholds on the generated QTd trend visually. By setting the threshold to 70% we ended up with more continuous QTd trends. The rejected leads were checked visually for 5 patients. We have observed a high correlation between the number of beats detected and the reliability of the measures taken within the defined interval.
The mean values of each remaining QTd_{ij}'s are calculated as:

$$\overline{QTdij[n]} = \frac{\sum^{n \in I_s \text{ and } QTdij[n] \neq -1} QTd_{ij}}{number\ of\ valid\ measurements\ on\ I_s}$$

Then we pick the five QTd_{ij}'s with highest mean values. Our aim is to select lead pairs with highest difference in QT intervals. The QTd trend is defined as the average of these five QTd_{ij}'s.

We use the same set of leads, which is selected previously for calculating QTd, to calculate Q-Tpk dispersion trends (QTpkd trends). Similarly, we define a set of Q-Tpk difference vectors as follows:

$$QTpkd_{ij}(n) = \begin{cases} QTpk_i(n) - QTpk_j(n) & \text{if } QTpk_i(n) \neq \text{-1 and } QTpk_j(n) \neq \text{-1} \\ -1 & \text{o.w} \end{cases}$$

We then calculate the mean values of these Q-Tpk difference vectors as follows.

$$\overline{QTpkdij[n]} = \frac{\sum^{n \in I_s \text{ and } QTpkdij[n] \neq -1} QTpkd_{ij}}{number\ of\ valid\ T-peak\ measurements\ on\ I_s}$$

We define QTpkd as the average of the five Q-Tpk difference vectors with highest mean values.

The most common definition for QTd dispersion is $QTd = QT_{max} - QT_{min}$ This definition did not perform well in exercise ECG because this definition

uses different leads throughout the exercise. This resulted in inconsistency in the QTd trends (section 4.3). So we decided to use the same pair of leads throughout all the exercise. Figure 2.10 shows an example of generated QTd

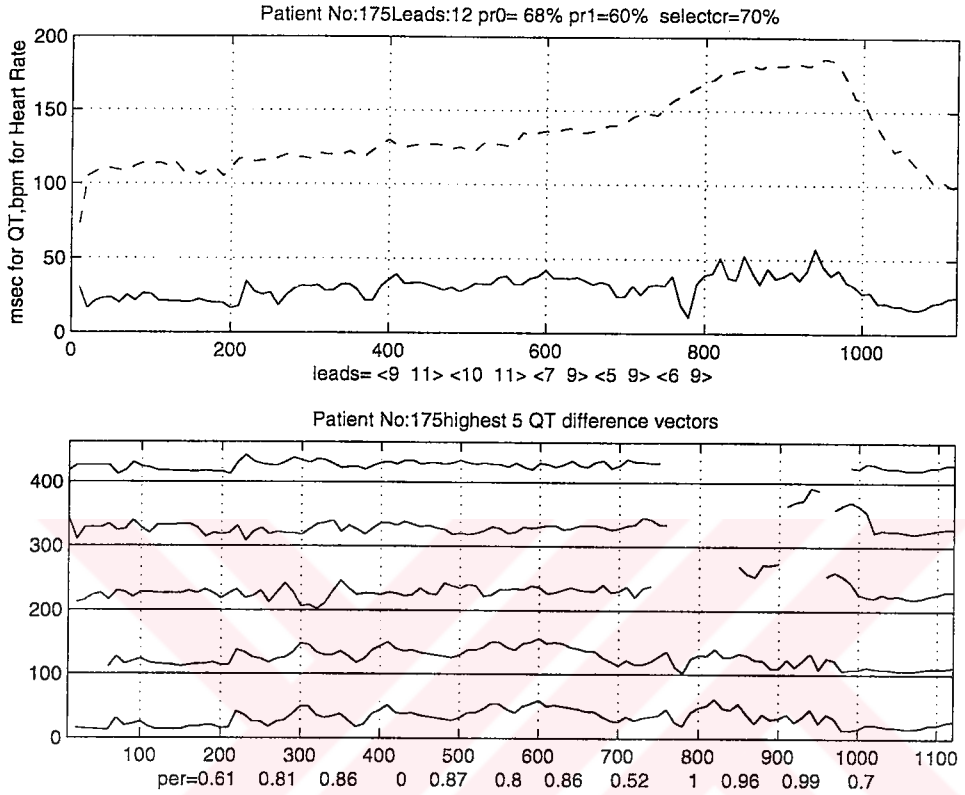

Figure 2.10: An example of QTd trend.

trend (top figure solid line). On the same figure the heart rate is plotted in dashed lines. The second graph shows the five difference vectors (QTd_{ij}'s) used for calculating the QTd trend. The first three QTd_{ij}'s show discontinuity around the exercise peak. This is due to critical TP fusion on leads 6,5 and 7. The numbers under the lowest figure in Figure 2.10 show the percentages of measurements that were possible for each lead. Leads 6,5 and 7 have less number of detected points than leads 9, 10 and 11 that's why $QTd_{6,9}$, $QTd_{5,9}$and

$QTd_{7,9}$ are discontinuous while $QTd_{9,11}$ and $QTd_{10,11}$ are not. From this example it is clear that using more than one difference vector provides more continuous QTd trends because when ever we fail to have any measurements on a vector it is more likely that we have a valid measurement at least on one of the other four. For this patient it was possible to detect QT end on 68% of the exercise test. An extra 8% was rejected during reliability checks. So the QTd trend was generated using only 60% of the exercise test.

2.4 Decision Making

We use a set of decision rules to differentiate between positive and negative QTd trends. A decision rule depends either on the characteristics of the generated QTd trends or on the relation between the QTd trends and the heart rate. In the following the proceeding terms are used: $QTpkd$: Trend generated using the T-peak, QTd: Trend generated using the T-end, (HR): Heart rate trend.

Correlation : We calculate the cross correlation coefficients (ccc) between $QTpkd$, QTd and the heart(HR) as follows:

$$ccc1 = \frac{\sum_{\substack{i=1,QTd(i)\neq -1 \\ and\ QTpkd(i)\neq -1}}^{l} QTd(i)QTpkd(i)}{\sqrt{\sum_{\substack{i=1,QTd(i)\neq -1 \\ and\ QTpkd(i)\neq -1}}^{l} QTpkd^2(i).\sum_{\substack{i=1,QTd(i)\neq -1 \\ and\ QTpkd(i)\neq -1}}^{l} QTd^2(i)}} \tag{2.9}$$

$$ccc2 = \frac{\sum_{\substack{i=1,QTd(i)\neq -1 \\ and\ HR(i)\neq -1}}^{l} QTd(i)HR(i)}{\sqrt{\sum_{\substack{i=1,QTd(i)\neq -1 \\ and\ HR(i)\neq -1}}^{l} HR^2(i).\sum_{\substack{i=1,QTd(i)\neq -1 \\ and\ HR(i)\neq -1}}^{l} QTd^2(i)}} \tag{2.10}$$

$$ccc2 = \frac{\sum_{\substack{i=1,QTpkd(i)\neq -1 \\ and\ HR(i)\neq -1}}^{l} QTpkd(i)HR(i)}{\sqrt{\sum_{\substack{i=1,QTpkd(i)\neq -1 \\ and\ HR(i)\neq -1}}^{l} HR^2(i).\sum_{\substack{i=1,QTpkd(i)\neq -1 \\ and\ HR(i)\neq -1}}^{l} QTpkd^2(i)}} \tag{2.11}$$

As heart rate increases the depolarization time between healthy and injured parts of the heart increases in ischemic patients. It was reported in previous studies [7] [8] that this will lead to an increase in QTd trends and QTd measures for patients with ischemic heart disease. Such changes are expected to lead to higher cross correlation coefficient between the QTd trends and the heart rate. We also calculate the cross correlation between the trends of the T-peak and the T-end dispersions in order to investigate the relation between the two measures and its variation for different patients.

Threshold : We can assign a single threshold value, instead of investigating the entire behavior of the QTd trend. We calculate the QTd maximum range for all trends as follows:

$$mx_{QTd} = QTdT_{end_{MAX}} - QTdT_{end_{MIN}} \tag{2.12}$$

$$mx_{QTpkd} = QTdT_{pk_{MAX}} - QTdT_{pk_{MIN}} \tag{2.13}$$

We report a patient positive if either mx_{QTd} or mx_{QTd} exceeds a certain threshold value.

Slope : We fit two least square lines L_{ex} and L_{re} respectively to the recovery and the exercise phases of the QTd trends. We then determine the slopes of the lines S_{ex} and S_{res}. We define S as the absolute sum of the two slopes. We expect higher values of S for QTd positive trends.

Chapter 3

EXPERIMENTS

3.1 Data Set

We use ECG test data for 54 different patients for this study. The raw exercise ECG data recordings for these patients were obtained at the Eskisehir hospital through the use of the Kardisosis PC based exercise ECG system. For each patient 12 leads ECGs were recorded during a Bruce Protocol based exercise test with a sampling rate of 500 samples/sec and at a 2.9-microvolt resolution. We also use a different data set of 24 patients for decision rule evaluation. Four of these patients had coronary angiography results, which is an invasive diagnostic tool for ischemic heart disease. Only one of these patients was reported non-ischemic. A qualified cardiologist examined ST plots, which represent a non-invasive tool for ischemia diagnosis, for all 24 patients. Twelve of these patients were reported ST positive.

3.2 Analysis

The software Efor from TEPA is used for averaging and filtering. The algorithm for fiducial point detection is developed using Borland C whereas the algorithm for producing QTd trends is implemented using Matlab.

We process the data for the 78 patients using those programs. We obtain 78 different QTd trends. Since the first data set was not clinically verified we have only used QTd trends from the second data set for our analysis (Appendix A). A decision is made on this data and the results are compared with clinical data. Throughout the development and analysis of ECG features the viewer software of Massachusetts Institute of Technology (MIT) and Beth Israel Hospital (BIH) had been used for checking visually the detected fiducial points. We have developed another program using Matlab for checking parabola fitting and T-end detection.

3.3 Results

The generated QTd trends do not show any significant variation with increasing exercise (Appendix A). For some patients, we have noticed some slight increase in QTd trends generated using 0% rejection ratio. On the other hand, the QTd trends generated using 70% rejection ratio for the same patients, do not show any significant changes. We have verified the rejected leads visually. We have noticed that the measurements for these leads are not reliable and are most of the time biased by a high TP fusion.

We have used a specificity-sensitivity test [9] for all proposed decision rules.

The results of the test are shown in Appendix B.

$$Sensitivity = \frac{True\ Positives}{True\ positives + False\ negatives}$$

$$Specificity = \frac{True\ Negatives}{True\ positives + False\ negatives}$$

We have calculated the area under the Receiver Operator Characteristics (ROC) curve (Table 3.1). The maximum value measured is 76%. It is measured using the maximum QTd trend difference. The rest of the decision rules show lower percentage area values.

Decision rule	Percentage area under the ROC curve
ccc1($QTpkd$ and QTd)	51.7%
ccc2(HR and QTd)	30 %
ccc3(HR and $QTpkd$)	42%
mx_{QTd}	76%
mx_{QTpkd}	40%
S(slope)	55%

Table 3.1: Results of the Specificity-Sensitivity Test

Chapter 4

DISCUSSION

4.1 Significance of the QTd Trends and the Decision Rules as a Discriminative Factor between Healthy and Cardiac Subjects:

Neither the generated QTd trends nor the associated decision rules are discriminative between cardiac and healthy patients. The low correlation between the QTd and the ST segment analysis propose that both tools are measuring different characteristics of the exercise ECG. Unlike T-end measurement, determining the ST level is less problematic, which may explain the reliability of this measure as diagnosis tool. In our study the number of patients with angiography results is limited (only four patients). As a future work it is important to investigate the QTd behavior on a larger population with clinically verified data.

4.2 Comparison between the Least Square Line Fit (LSF) and the Least Square Parabola Fit (LSPF) Algorithms:

The LSF algorithm introduced earlier was reported to be more reproducible than any other QT-end detection algorithm [1]. For comparing our algorithm (LSPF) with the LSF algorithm and due to the absence of reproducible data we use a linear regression test. For conducting this test we use exercise test data from 15 different patients (11550 QRS complexes). The statistics of the measurements are shown in Table 4.1:

	All measurements	Rest measurements
Total number of beats	11550	330
Number of beats on which LSPF failed	3830	138
Number of beats on which LSI failed	5010	158
Number of beats on which both algorithms failed	3575	135
	Mean	Std
LSPF	307.9 (msec)	38.22
LSF	321.4(msec)	39.22

Table 4.1: Statistical comparision between the LSF and LSPF algorithms

An algorithm fails when it does not succeed to determine a T-end for a certain average beat. The criteria of failure depend on both the algorithm performance and the signal quality. According to the statistics the LSF failed on 47% of the rest measurements and on 43.8% of the total number of measurements. On the other hand, the LSPF algorithm failed on 41% of the rest

measurements and on 33.16% of the total number of measurements. The measured T-end's were verified visually. We have noticed that the T-end values measured using the LSF algorithm are higher (mean=321.4 milliseconds) than the T-end values measured using the LSPF algorithm (mean=307.9 milliseconds). This can be explained by the fact that in the LSF algorithm we fit our line to the maximum derivative point while in the LSPF algorithm our line is fitted to the 80% of absolute parabola maximum level. That is, the slope of the fitted lines and the points to which the lines are fitted are different in both algorithms. A plot of the QT intervals measured by the LSF algorithm versus QT intervals measured using the LSPF algorithm is shown in Figure 4.1.

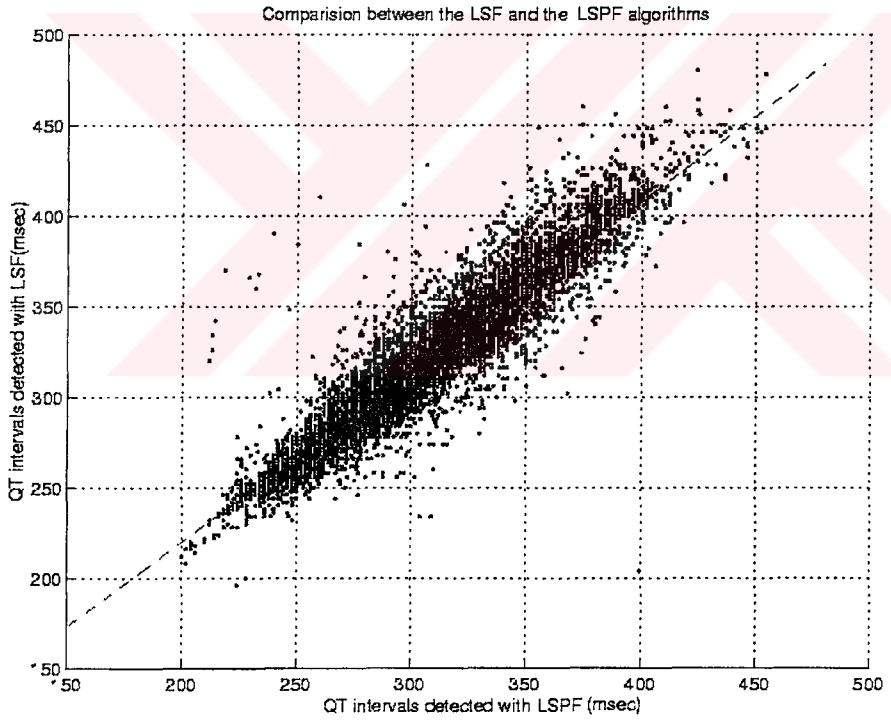

Figure 4.1: Comparision between the LSF and the LSPF algorithms.

The shape of the graph proposes that both algorithms are measuring the same characteristics of the average beat. A least square line is fitted to the data. The parameters of the line are slope = 0.94 and x-axis intersect = 31.86. To investigate the difference between the two algorithms we have to consider the outliers. These correspond to average beats where both algorithms detect significantly different T-peaks for the same average beats. After visual verification we have noted that the shape of the falling edge of the T wave varies between successive beats due to several artifacts. The LSPF algorithm is more robust to these variations. This is mainly because the LSPF algorithm uses more sample points than the LSF algorithm. This makes it more stable to noise and regional changes effecting the falling edge of the T wave.

4.3 Comparison of our QTd Definition with Previous Definitions

In this section we compare our QTd definition with other QTd definitions appearing in literature. We take into consideration the following definitions: Range (QTdc), Standard deviation (SD) and Interquartile range (IQR). We have generated QTd trends for all four definitions (Figure 4.2). The classical definition shows a very noisy QTd trend. This is due to the fact that the classical definition uses different pair of leads for different time instants while our definition calculates QT difference for the same lead pairs throughout all exercise.

The statistics in Table 4.2 show that the QT dispersion values vary significantly throughout exercise and recovery phases for all three definitions. This

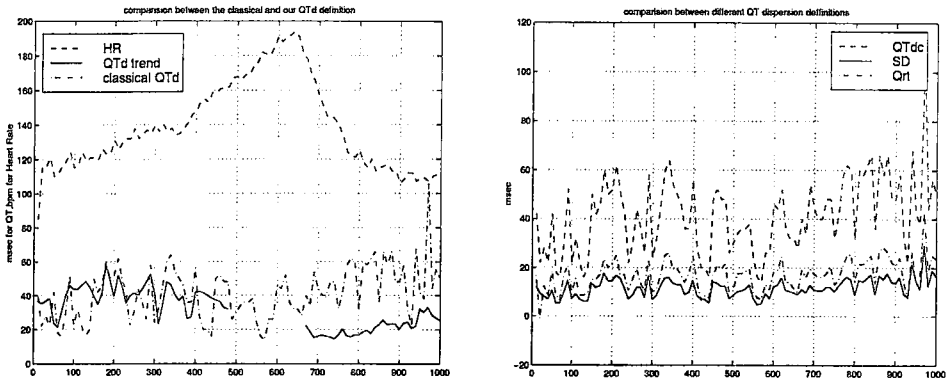

Figure 4.2: QTd trends generated by different QT dispersion formulae.

suggests that using a single value of QTd dispersion for exercise does not reflect the entire behavior of the heart, moreover if this value is selected at exercise peak [5] it is less reliable due to the effect of TP fusion on QTd end measurements. In some studies corrected QT dispersion was used [4]. The QT

QTd definition	Range	Standard deviation	Interquartile range
Rest QTd	42	12.15	16.5
QTd range(exr)	50	12.9	20
Mean(exr)	36.7	10.54	15.15
SD(exr)	13.82	3.43	5.77
QTd range(rec)	46	21	35
Mean(rec)	49.3	13.55	4.24
SD(rec)	15.98	19	6.62

Table 4.2: Comparision between different QTd formulae

correction formulae were derived for canceling the effect of different heart rates when comparing QT intervals from different patients at rest. These formulae were generated for heart rates less then 120 bpm, hence we think it is an appropriate to use them for exercise ECG.

4.4 Effect of TP Fusion on T-end and QTd Measurements:

It is known that T-end detection for exercise ECG is very critical. Though presence of noise and baseline wonder can highly effect the reliability of the measures, TP fusion can be considered the most important limitation for generating reliable QTd trends. The latter makes it difficult to investigate QTd behavior at most advanced stages of exercise where we expect higher level of ischemia. Due to The presence of TP fusion a number QT intervals is not measured. As heart rate increases the RR interval shortens and the P wave is gradually pushed towards the T-end. This means that leads with maximum QT interval are first effected by TP fusion. As exercise level increases no more measurements are possible on these leads and this is reflected by a gap in the QTd trend round the exercise peak. The omitted leads are expected to carry significant information since they are commonly the leads leading to maximum dispersion. As future work it seems necessary to develop more efficient algorithms that can deal with TP fused beats:

Chapter 5

CONCLUSION

QTd analysis is proposed as a non-invasive method for measuring dispersion of ventricular depolarization. At most three values, for rest, exercise, and recovery, of QTd dispersion were used in the previous studies. In our study we proposed a new approach for calculating QTd. Unlike previous studies we generate QTd trends for all exercise and recovery data. We defined these QTd trends on the same set of leads throughout all exercise and recovery phases. The set of leads on which we calculated the QTd trends were selected so that they give maximum amount of dispersion. We checked our QTd definition on data and we did improve it in order to eliminate the effect of noisy leads. We compared our QTd definition with classical QT dispersion definitions. We showed that using the complete QTd trend is more reliable than using single sample points for QT dispersion. This is because the classical definitions, which use at most three values of the QTd trend, do not reflect the entire behavior of ventricular depolarization due to the variations in the QTd trends.

For calculating the QTd we used a new T-end detection algorithm (LSPF) which is based on fitting a parabola to the peak of the T wave and determining the T-end using the tangent to this parabola. We compared the performance of the algorithm with previous algorithms. Our algorithm proved more stable than any other T-end detection algorithm. This is mainly because the fitted parabola to the T wave is mathematically well defined and fitting a line to the falling edge of the parabola is less problematic then fitting a line to the falling edge of the T wave. However, our algorithm is not immune to TP fusion and a big set of leads was rejected due to critical TP fusion.

In our study our aim was to investigate QTd for ischemic patients but due to the lack of validated data we evaluated QTd using data collected from patients with general cardiac abnormalities. We evaluated our algorithm using 24 exercise ECG recordings, 12 from normal patients and 12 from cardiac patients. A qualified cardiologist evaluated this data using ST diagnosis tests. We conducted discrimination analysis on this data set. The following decision rules were evaluated: Cross correlation (CCC), Threshold, and Slope. We used Specificity-sensitivity measures for evaluating the efficiency of the decision rules. Despite the improvement in T-end detection, thus in QTd measurements, the ROC curve analysis showed that QTd during exercise is not a clinically valuable discriminate of cardiac patients. The threshold decision achieved the maximum ROC curve area and it was 76%.

As future work I suggest that our algorithm be evaluated in a larger and clinically verified data set. The diagnosis of the patients in such a data set must be done by clinical means, like angiography. The results presented in this thesis are mainly a comparison of the clinically validated ST diagnosis tool and

our proposed QTd algorithm. TP fusion should also be further investigated in order to reduce the effect of missing leads on the calculated QT dispersion.

Finally, we should point out that the importance of cooperating with a hospital clinic in biomedical engineering research, which requires validated clinical data, could not be overemphasized. This project also required clinically validated exercise ECG records obtained in clinical environment. We tried to cooperate with many local cardiology clinics, and eventually agreed on a particular protocol (this protocol involved classification of patients according to gender, age and other validated test information), with a clinic in Iskisheir. However, it was again not possible to have the clinic implementation of this protocol. This situation is common, probably without any exception, and is well known among researchers in biomedical engineering who need to work on validated clinical data in this country. We believe that the current situation presents limitation for further development of the field of biomedical engineering science.

APPENDIX A

QTd Trends Plots

These are the QTd trends generated for 24 patients. For each patient two different sets of trends are generated. One with a rejection ratio $Rej = 70\%$, that is only leads with more then 70% detections in I_s were selected (see section). For the second set all leads were included for generating the QTd trends($Rej = 0\%$). 'A' stands for the angiography results and 'ST' for the ST diagnosis results.

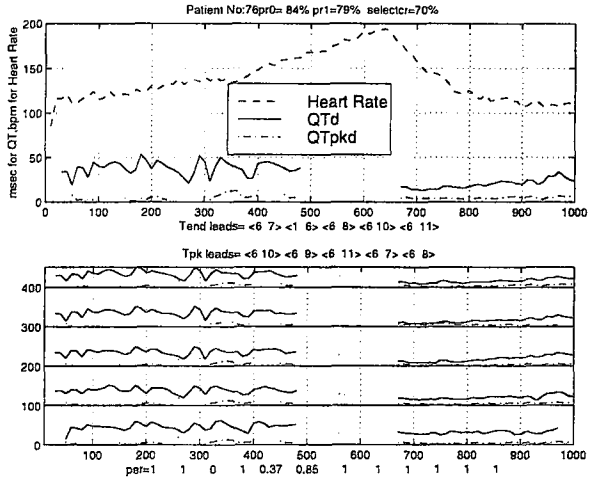

Figure A.1: QTd, QTpkd and Heart Rate for patient 76 ST=- A=? Rej=70%.

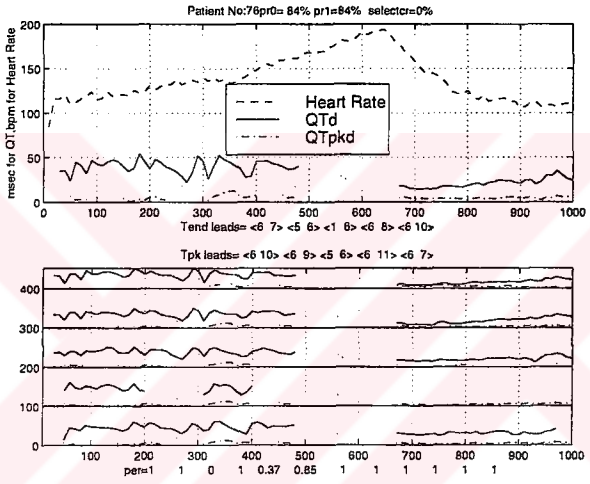

Figure A.2: QTd ,QTpkd and Heart Rate for patient 76 ST=- A=? Rej=0%.

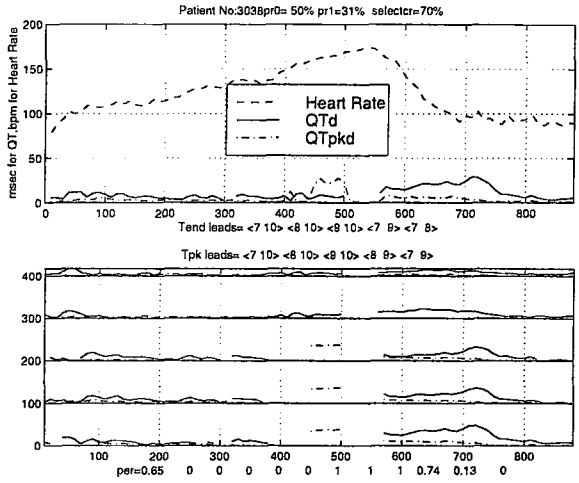

Figure A.3: QTd, QTpkd and Heart Rate for patient 3038 ST=- A=? Rej=70%.

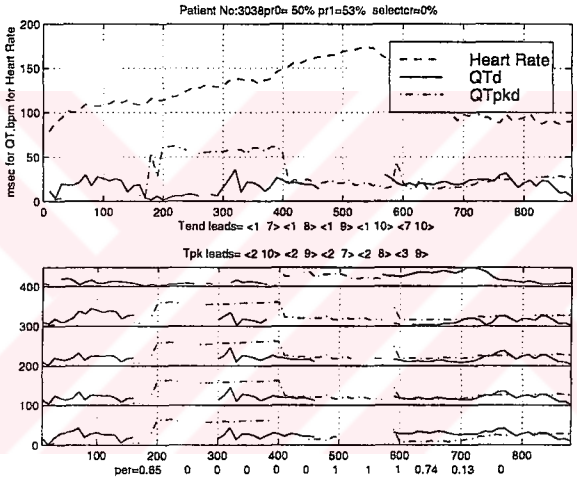

Figure A.4: QTd, QTpkd and Heart Rate for patient 3038 ST=- A=? Rej=0%.

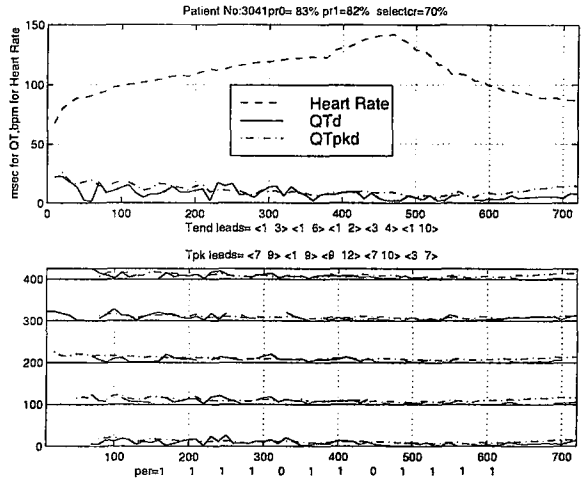

Figure A.5: QTd, QTpkd and Heart Rate for patient 3041 ST=- A=? Rej=70%.

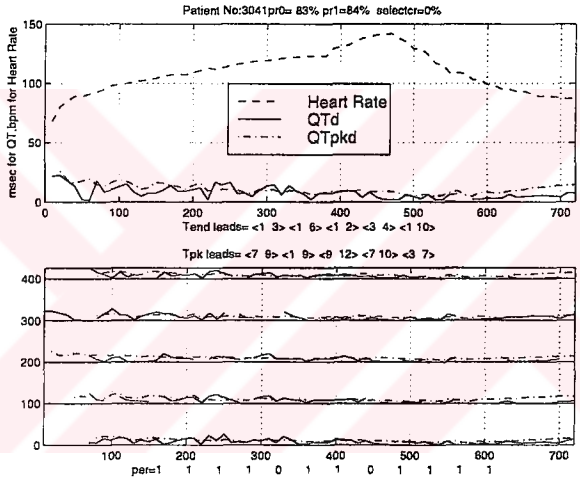

Figure A.6: QTd, QTpkd and Heart Rate for patient 3041 ST=- A=? Rej=0%.

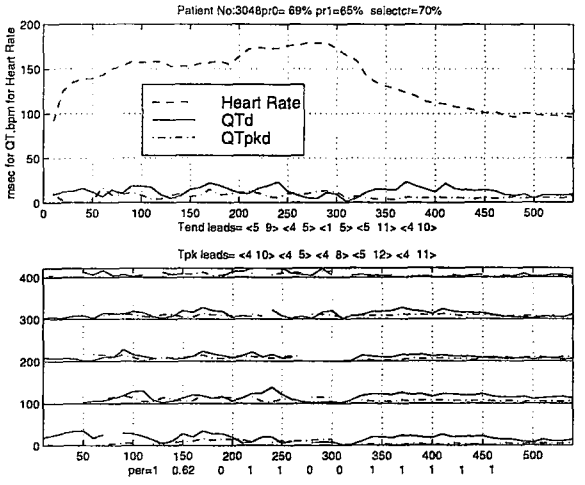

Figure A.7: QTd, QTpkd and Heart Rate for patient 3048 ST=- A=? Rej=70%.

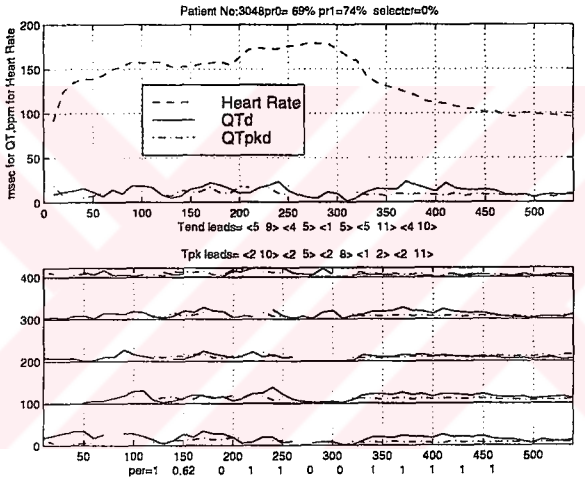

Figure A.8: QTd, QTpkd and Heart Rate for patient 3048 ST=- A=? Rej=0%.

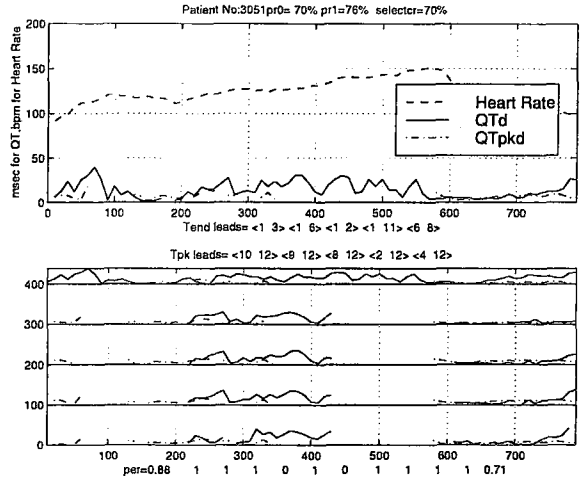

Figure A.9: QTd, QTpkd and Heart Rate for patient 3051 ST=- A=? Rej=70%.

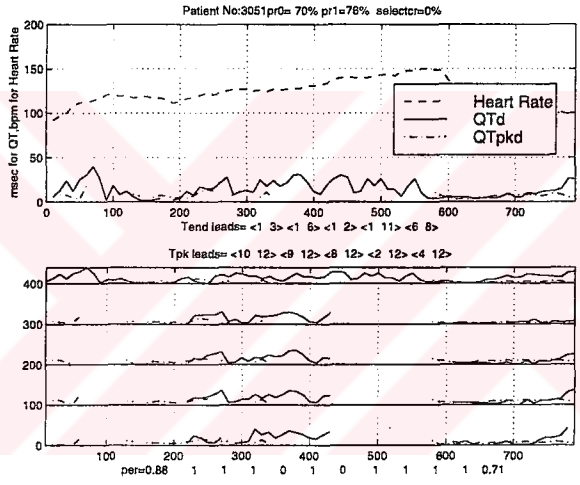

Figure A.10: QTd, QTpkd and Heart Rate for patient 3051 ST=- A=? Rej=0%.

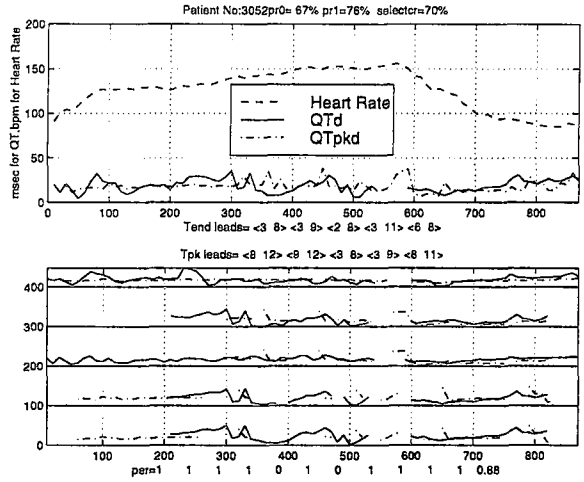

Figure A.11: QTd, QTpkd and Heart Rate for patient 3052 ST=- A=? Rej=70%.

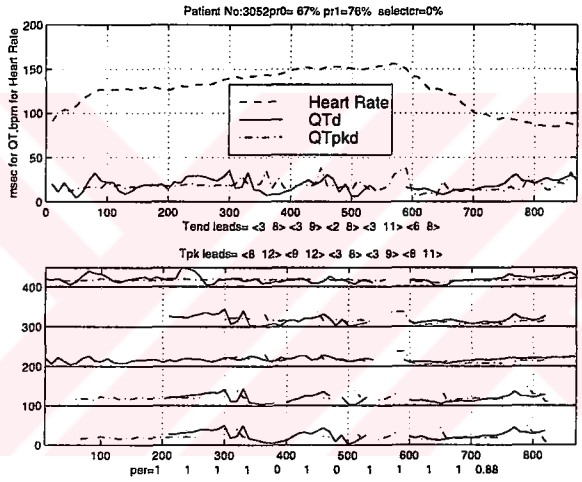

Figure A.12: QTd, QTpkd and Heart Rate for patient 3052 ST=- A=? Rej=0%.

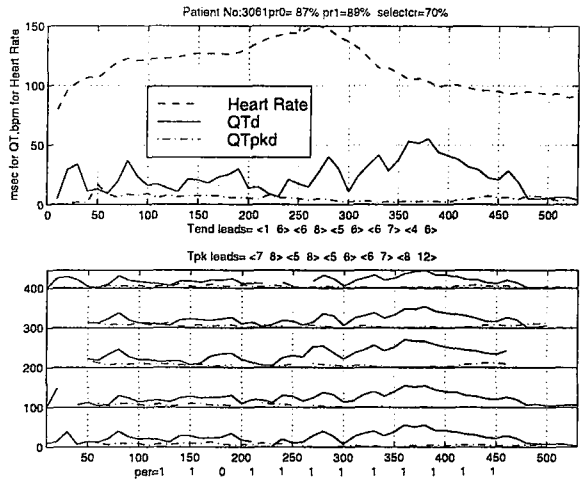

Figure A.13: QTd, QTpkd and Heart Rate for patient 3061 ST=- A=? Rej=70%.

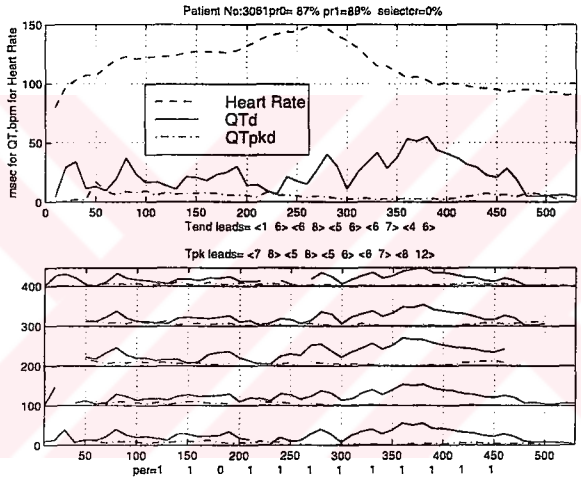

Figure A.14: QTd, QTpkd and Heart Rate for patient 3061 ST=- A=? Rej=0%.

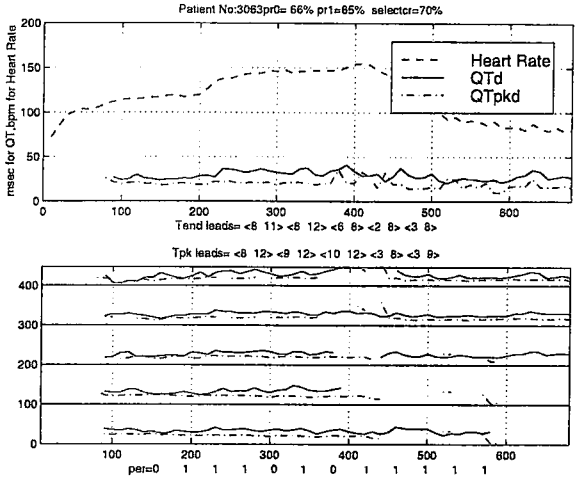

Figure A.15: QTd, QTpkd and Heart Rate for patient 3063 ST=- A=? Rej=70%.

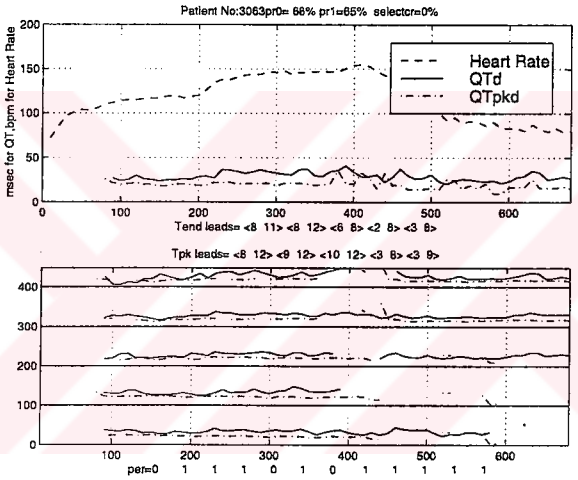

Figure A.16: QTd, QTpkd and Heart Rate for patient 3063 ST=- A=? Rej=0%.

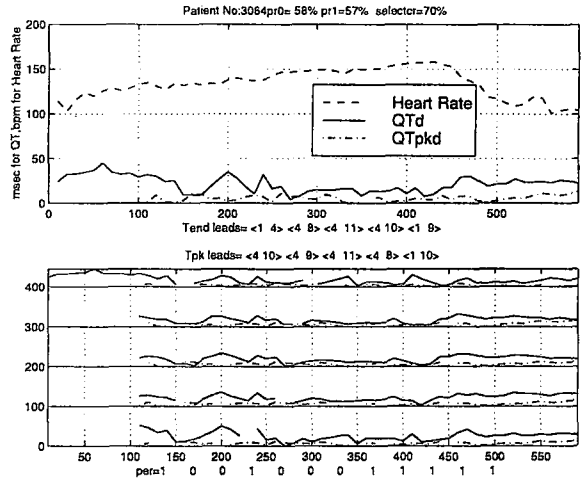

Figure A.17: QTd, QTpkd and Heart Rate for patient 3064 ST=- A=? Rej=70%.

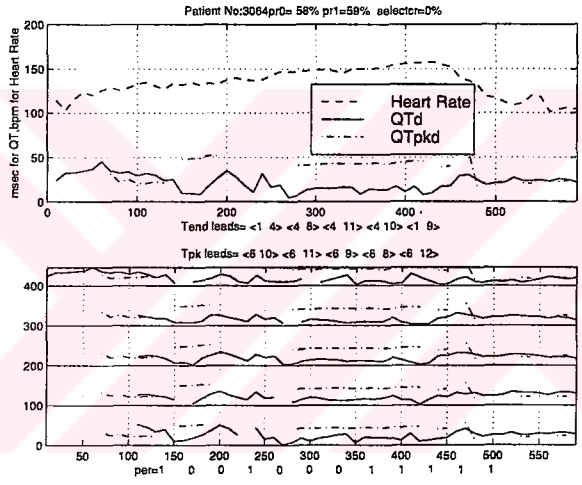

Figure A.18: QTd, QTpkd and Heart Rate for patient 3064 ST=- A=? Rej=0%.

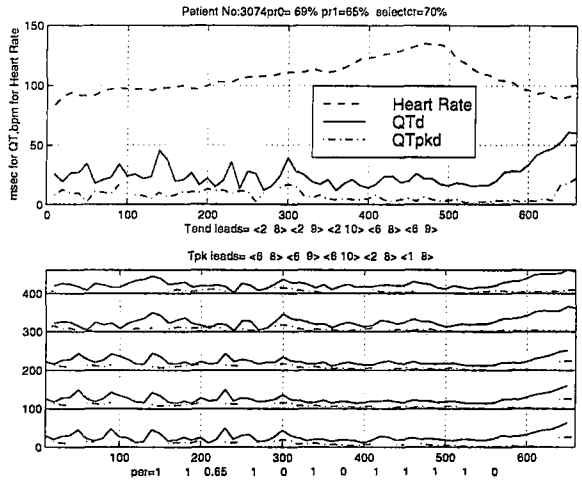

Figure A.19: QTd, QTpkd and Heart Rate for patient 3074 ST=- A=? Rej=70%.

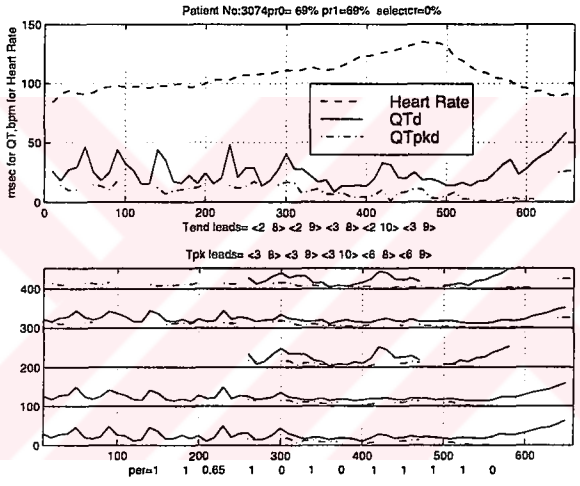

Figure A.20: QTd, QTpkd and Heart Rate for patient 3074 ST=- A=? Rej=0%.

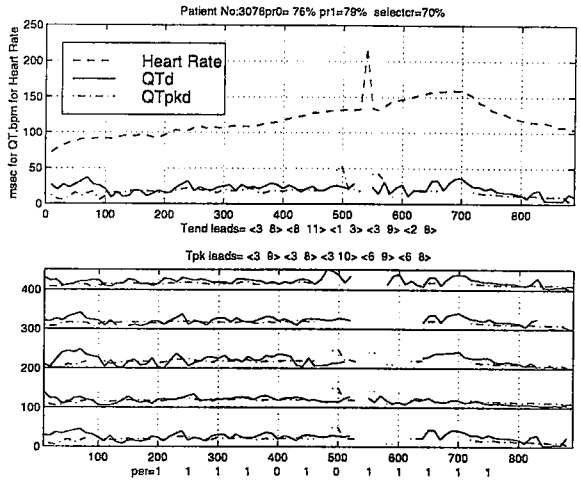

Figure A.21: QTd, QTpkd and Heart Rate for patient 3076 ST=- A=? Rej=70%.

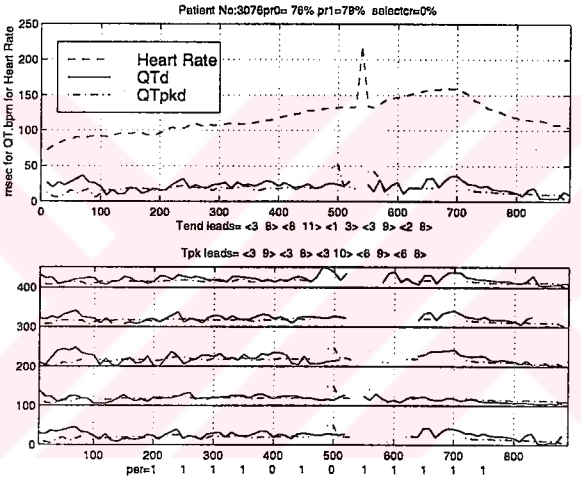

Figure A.22: QTd, QTpkd and Heart Rate for patient 3076 ST=- A=? Rej=0%.

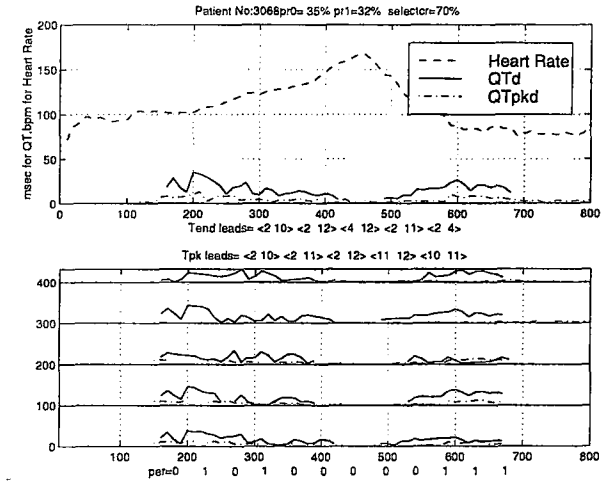

Figure A.23: QTd, QTpkd and Heart Rate for patient 3068 ST=+ A=- Rej=70%.

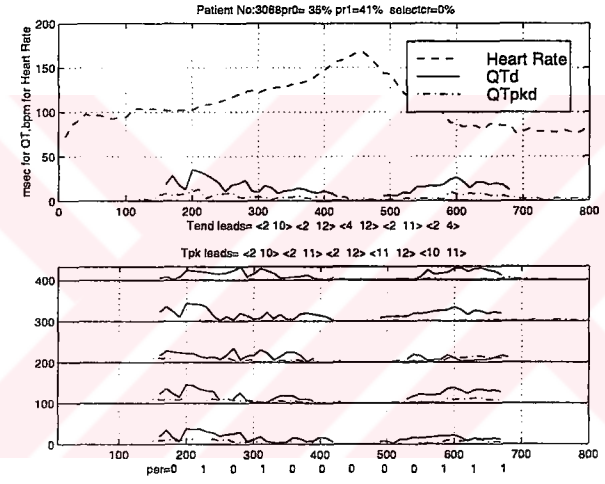

Figure A.24: QTd ,QTpkd and Heart Rate for patient 3068 ST=+ A=- Rej=0%.

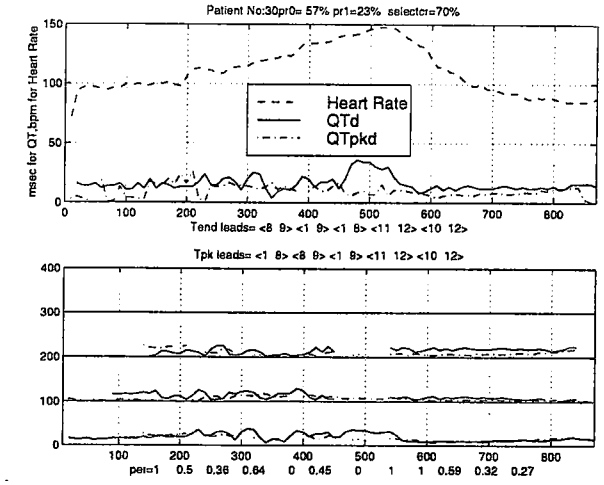

Figure A.25: QTd, QTpkd and Heart Rate for patient 30 ST=+ A=+ Rej=70%.

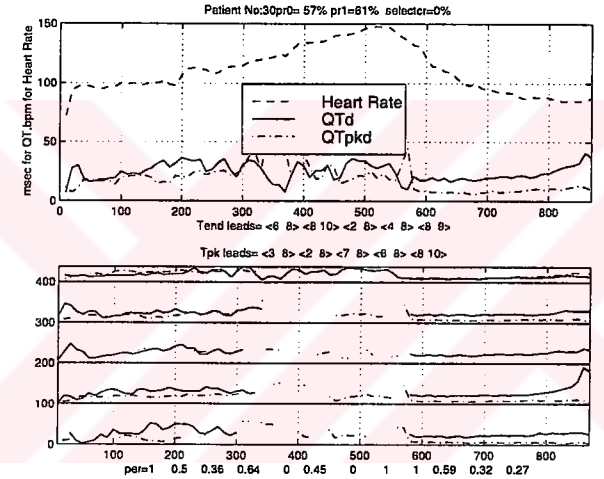

Figure A.26: QTd, QTpkd and Heart Rate for patient 30 ST=+ A=+ Rej=0%.

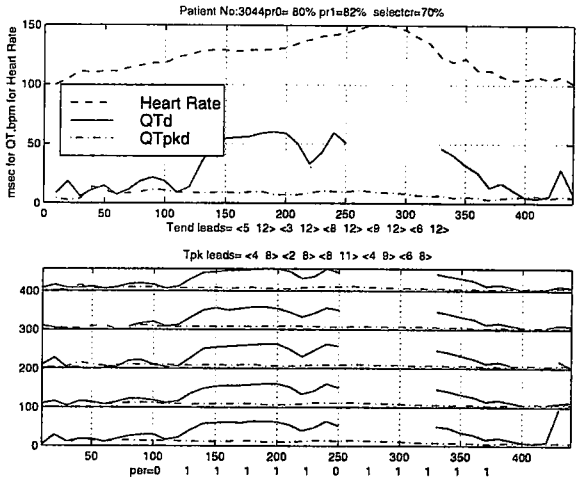

Figure A.27: QTd ,QTpkd and Heart Rate for patient 3044 ST=+ A=+ Rej=70%.

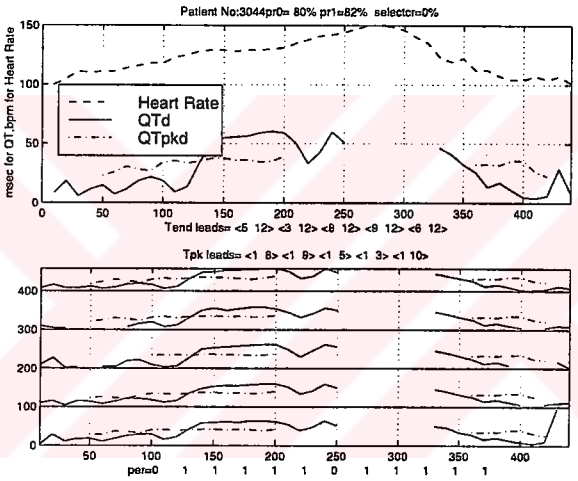

Figure A.28: QTd, QTpkd and Heart Rate for patient 3044 ST=+ A=+ Rej=0%.

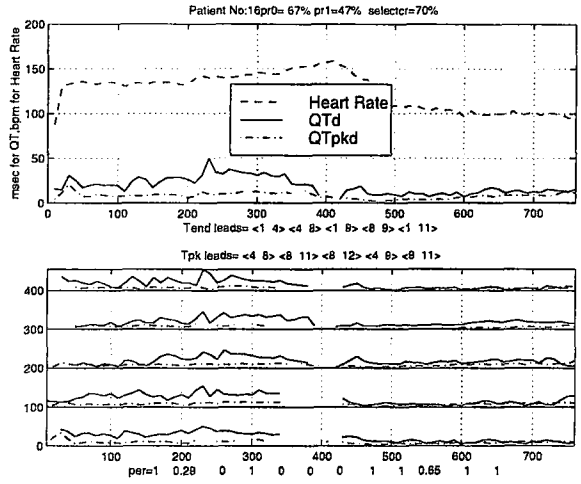

Figure A.29: QTd, QTpkd and Heart Rate for patient 16 ST=+ A=? Rej=70%.

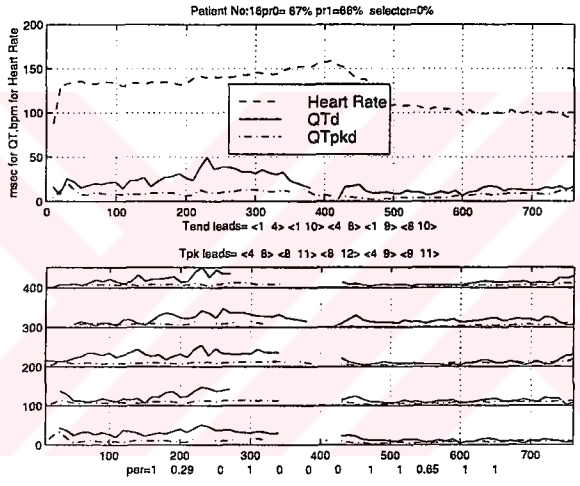

Figure A.30: QTd ,QTpkd and Heart Rate for patient 16 ST=+ A=? Rej=0%.

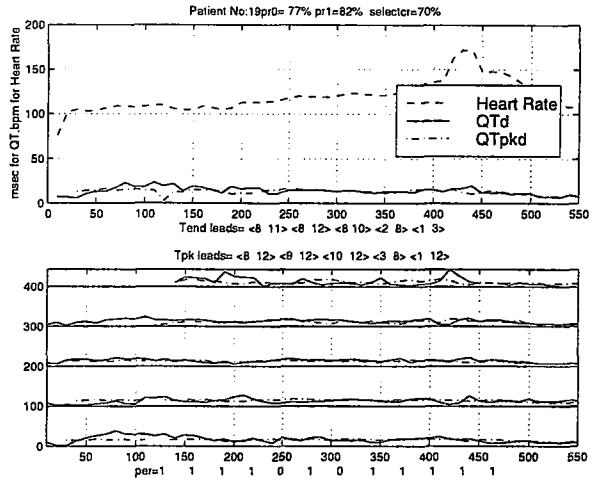

Figure A.31: QTd ,QTpkd and Heart Rate for patient 19 ST=+ A=? Rej=70%.

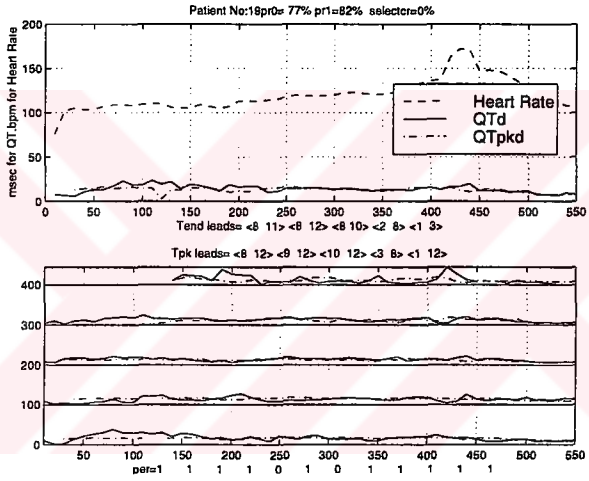

Figure A.32: QTd, QTpkd and Heart Rate for patient 19 ST=+ A=? Rej=0%.

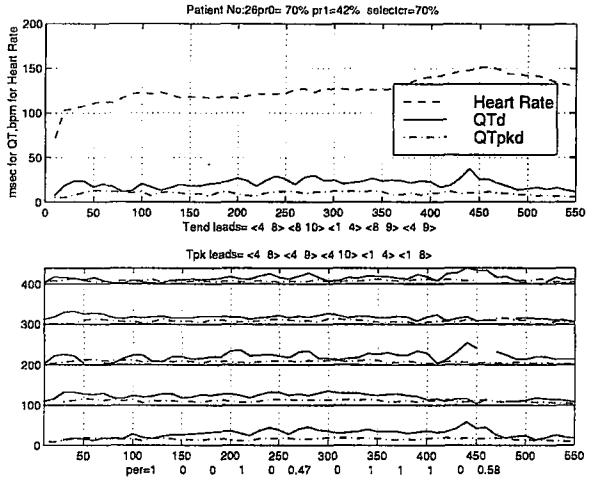

Figure A.33: QTd, QTpkd and Heart Rate for patient 26 ST=+ A=? Rej=70%.

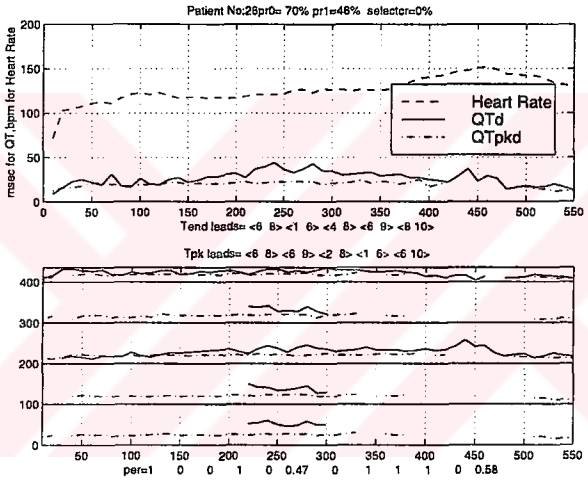

Figure A.34: QTd, QTpkd and Heart Rate for patient 26 ST=+ A=? Rej=0%.

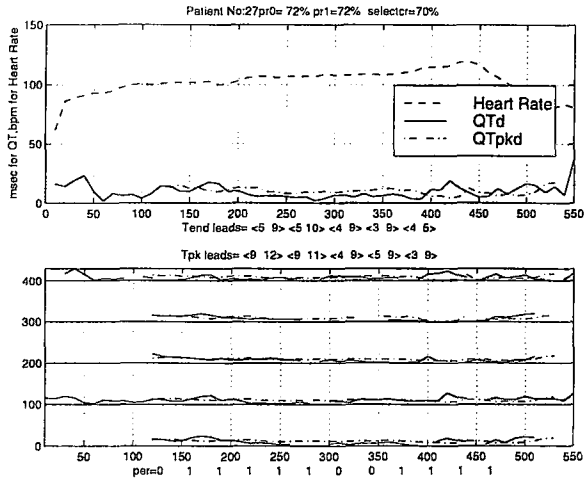

Figure A.35: QTd, QTpkd and Heart Rate for patient 27 ST=+ A=? Rej=70%.

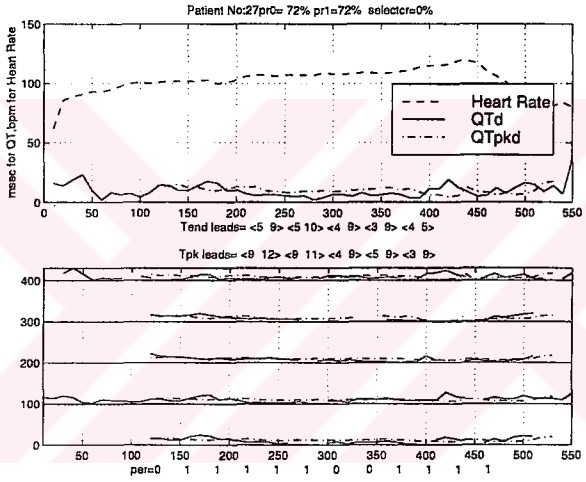

Figure A.36: QTd, QTpkd and Heart Rate for patient 27 ST=+ A=? Rej=0%.

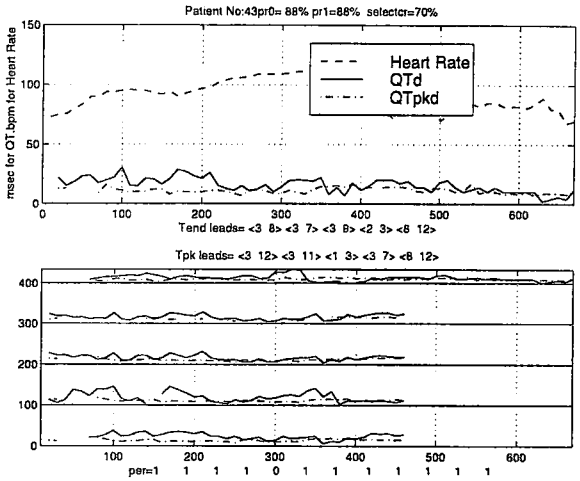

Figure A.37: QTd, QTpkd and Heart Rate for patient 43 ST=+ A=? Rej=70%.

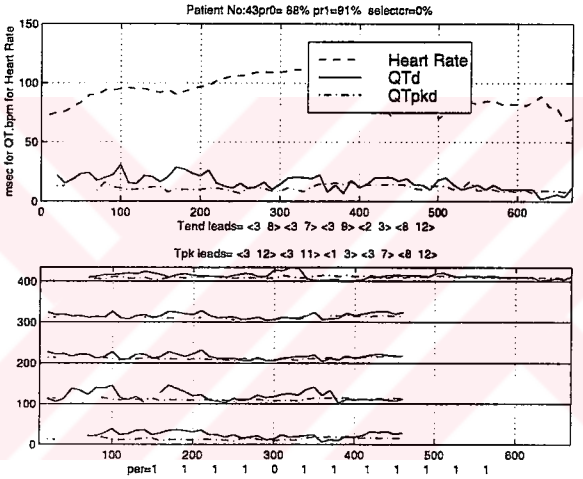

Figure A.38: QTd, QTpkd and Heart Rate for patient 43 ST=+ A=? Rej=0%.

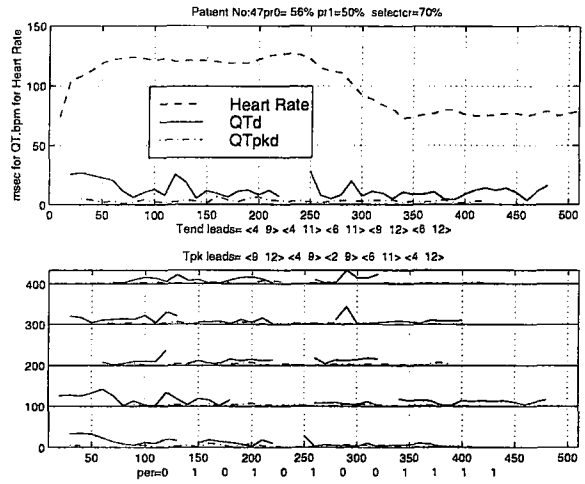

Figure A.39: QTd ,QTpkd and Heart Rate for patient 47 ST=+ A=? Rej=70%.

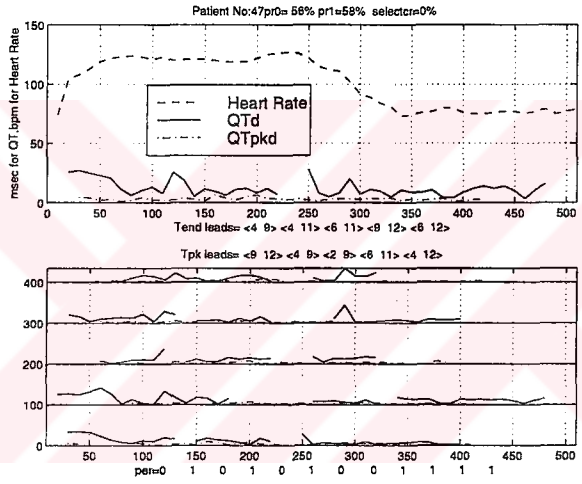

Figure A.40: QTd, QTpkd and Heart Rate for patient 47 ST=+ A=? Rej=0%.

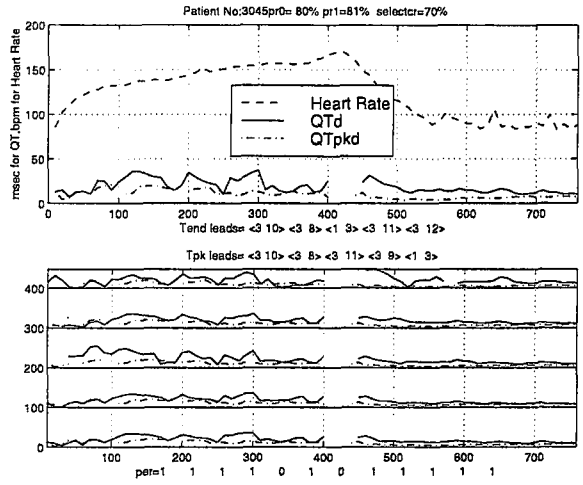

Figure A.41: QTd, QTpkd and Heart Rate for patient 3045 ST=+ A=? Rej=70%.

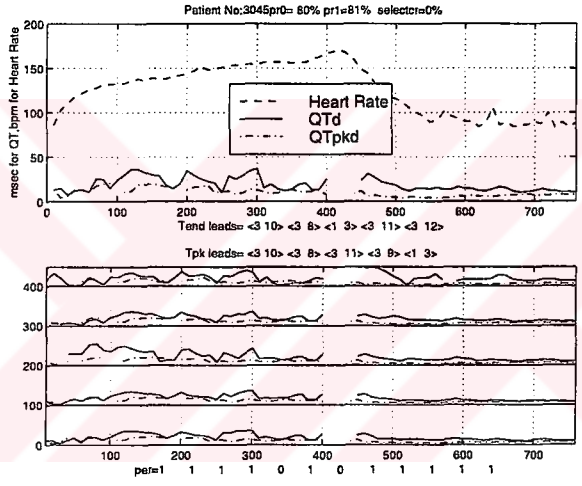

Figure A.42: QTd, QTpkd and Heart Rate for patient 3045 ST=+ A=? Rej=0%.

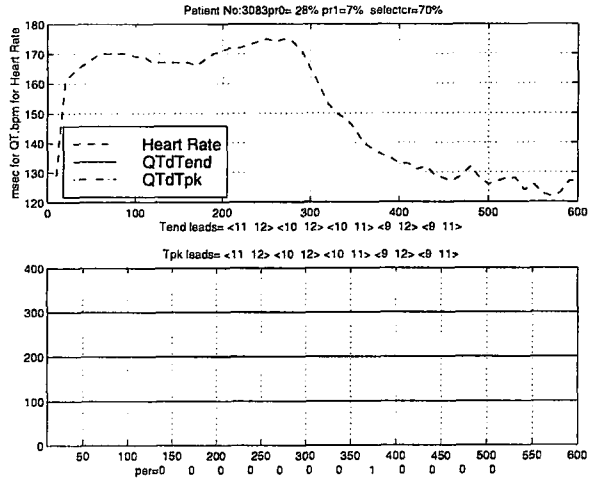

Figure A.43: QTd, QTpkd and Heart Rate for patient 3083 ST=+ A=? Rej=70%.

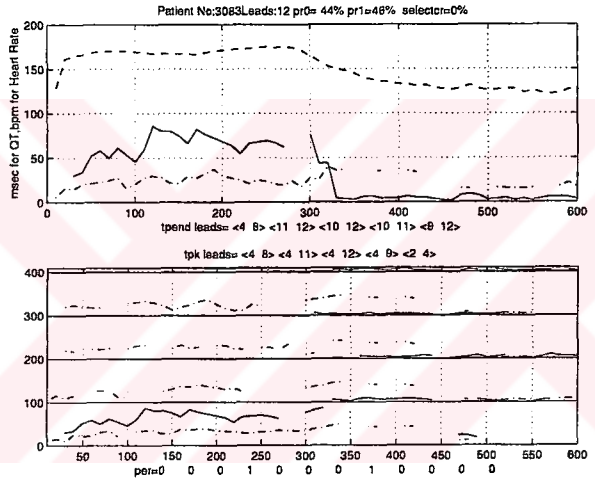

Figure A.44: QTd, QTpkd and Heart Rate for patient 3083 ST=+ A=? Rej=0%.

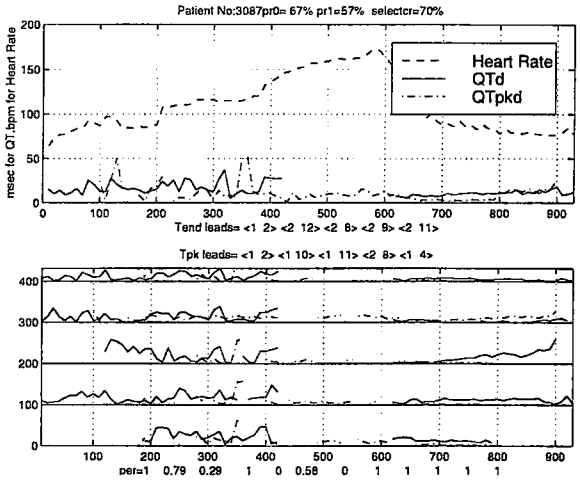

Figure A.45: QTd, QTpkd and Heart Rate for patient 3087 ST=+ A=? Rej=70%.

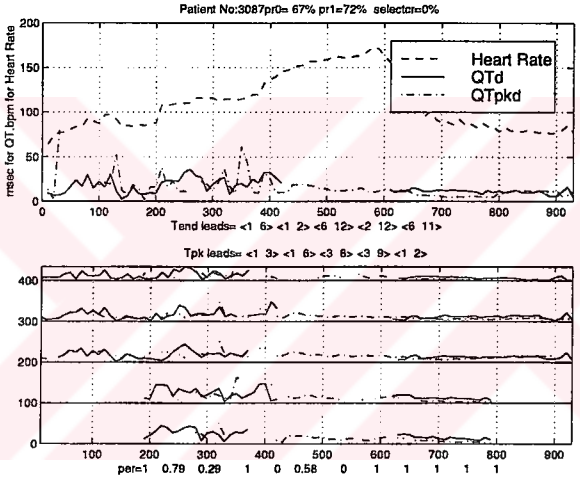

Figure A.46: QTd, QTpkd and Heart Rate for patient 3087 ST=+ A=? Rej=0%.

APPENDIX B

Decision rules evaluation

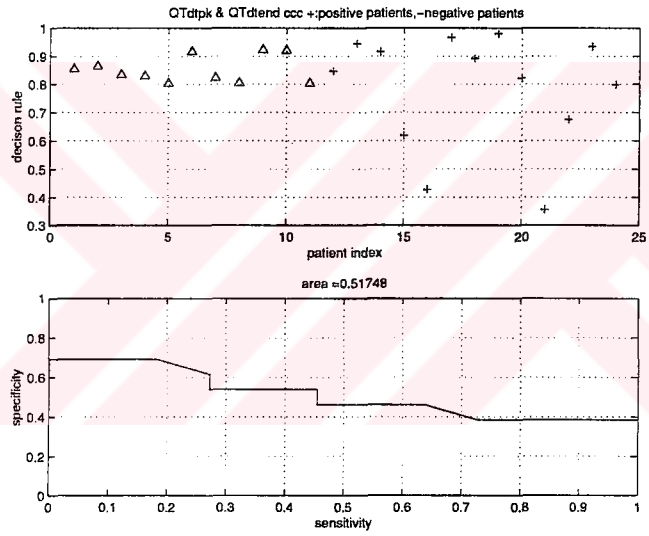

Figure A.1: QTpkd QTd ccc.

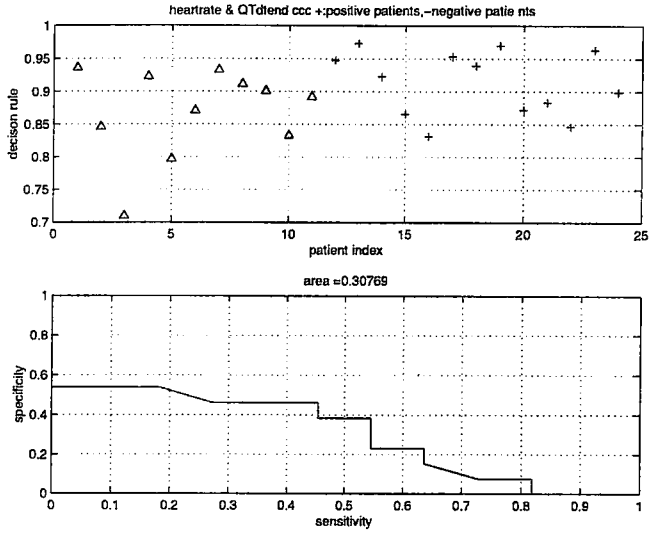

Figure A.1: Heart rate QTd ccc.

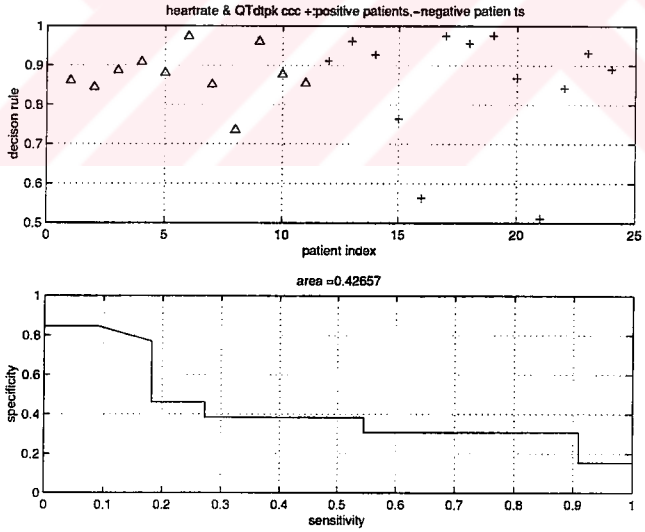

Figure A.2: Heart rate QTpkd ccc.

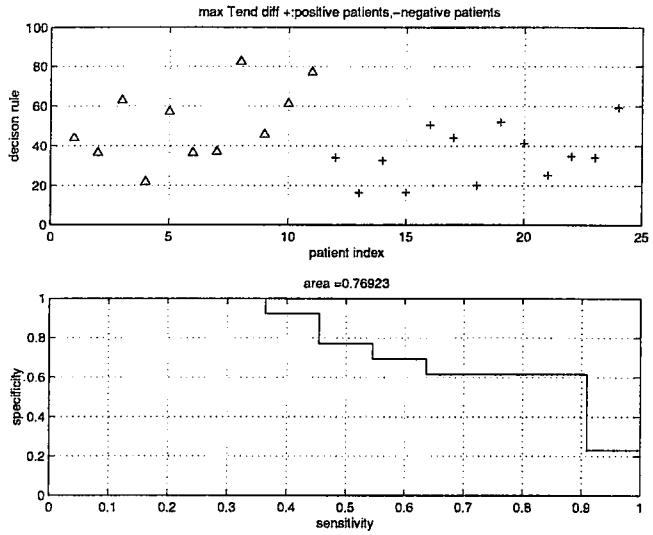

Figure A.3: QTd max difference.

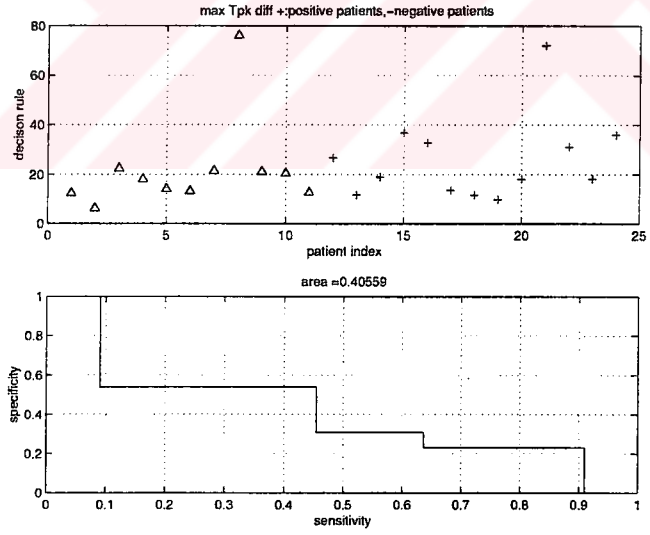

Figure A.4: QTpkd max difference.

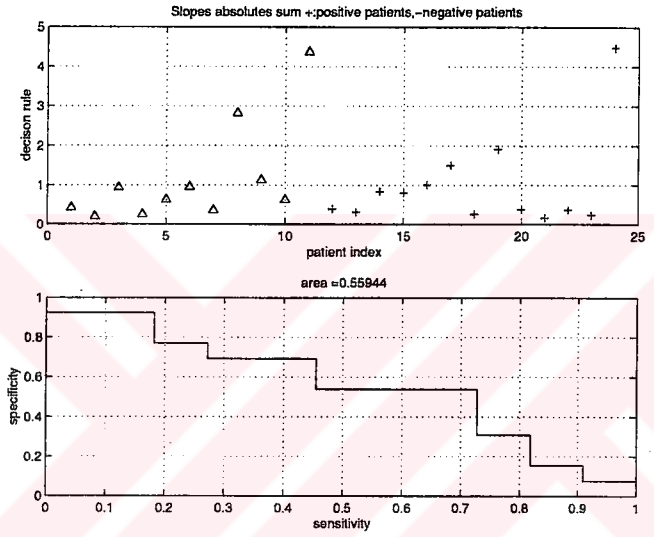

Figure A.5: Slope absolute sum.

Bibliography

[1] Q. Xue and S.Reddy, "New Algorithms for QT Dispersion Analysis," *Computers in Cardiology*,vol. 30, pp. 293–296, 1996.

[2] Q. Xue and S.Reddy, "Algorithms for computerized QT Analysis," *Journal of Electrocardiology. Supplement*, vol. 30, pp. 181–186, 1998.

[3] R. Plonsey and R.C. Barr, "Biolectricity, A Quantitative Approach," *PLENUM PRESS. NEW YORK AND LONDON*, pp. 218–219, 1991.

[4] Stoletniy LN, Pai RG, "Usefulness of QTc dispersion in interpreting exercise electrocardiograms," *AM Heart J*, vol. 130(4), pp. 918–921, 1995.

[5] G. Yi, R. Crook, X.H. Guo, A. Staunton,A.J. Camm, M.Malik, "Exercise-induced changes in the QT interval duration and dispersion in patients with sudden cardiac death after myocardial infarction ," *International Journal of Cardiology*, vol. 63, pp. 271–279, 1998.

[6] McLaughlin N., Campbell R., Murray A., "Comparision of automatic QT measurement techniques in the normal 12 lead electrocardiogram ," *Br Heart J*, vol. 74(4), pp. 84–89, 1995.

[7] L.Ozcakir, "EFFECT OF EXERCISE ON QT DISPERSION ," *A master thesis submitted to Faculty of Engineering and Science of Bilkent University*, December 1998.

[8] G. Tomasson ,E. Pisano,L. Gardner,W. Krucoff,A. Natale "QT Prolongation and Dispersion in Myocardial Ischemia and Infarction ," *Journal of Electrocardiology. Supplement*, vol. 30, pp. 187–190, 1998.

[9] S LN, Pai RG, "Computation of multifractorial receiver operator and predictive accuracy characteristics ," *Computer methods and Programs in Biomedecine*, vol. 42(4), pp. 147–156, 1994.

[10] N B McLaughlin, R W F Campbell, A Murray, "Accuracy of four automatic QT measurement techniques in cardiac patients and healthy subjects ," *Heart* , vol. 76, pp. 422–426, 1996.

[11] Bhullar HK, Fothergill JC, Goddard WP, et al."Automated measurement of QT interval dispersion from hard-copy ECGs," *J Electrocardiol* , vol. 26, pp. 321–31, 1993.

[12] Higham PD,Furniss SS, Campbell RWF."QT dispersion and components of the QT interval in ischemia and infarction," *Br Heart J* , vol. 73, pp. 32–36, 1995.

[13] Davey PP Bateman J, Mulligan IP, et al."QT interval dispersion in chronic heart failure and left ventricular hypertrophy: relation to autonomic nervous system and Holter tape abnormalities," *Br Heart J* , vol. 71, pp. 268–73, 1994.

[14] Hnatkova K, Malik M, Kautzner J, et al."Adjustment of QT dispersion assessed from 12 lead electrocardiograms for different numbers of analysed

electrocardiographic leads:comparision of stability of different methods," *Br Heart J*, vol. 74, pp. 676–9, 1995.

[15] P Langley, D di Bernado, A murray."Comparison of Three Measures of QT Dispersion," *Computers in Cardiology*, vol. 26, pp. 69–72, 1999.